

Protein Localization During the Cyanobacterial Circadian Cycle

by
Prashant Luitel

B.A., Physics (2005)

Reed College

Submitted to the Department of Physics
in Partial Fulfillment of the Requirements for the Degree of
Master of Science in Physics

at the

Massachusetts Institute of Technology

February 2008

©2008 Massachusetts Institute of Technology
All rights reserved

Signature of Author.....

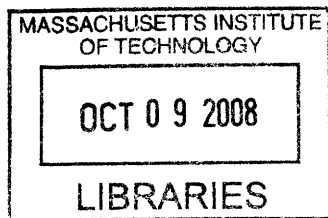
Department of Physics
January 24, 2008

Certified by

Alexander van Oudenaarden
Associate Professor of Physics
Thesis Supervisor

Accepted by.....

Thomas Greytak
Professor of Physics
Associate Department Head of Education



ARCHIVES

Protein Localization During the Cyanobacterial Circadian Cycle

by
Prashant Luitel

Submitted to the Department of Physics on January 24, 2008
in Partial Fulfillment of the Requirements for the
Degree of Master of Science in Physics

ABSTRACT

Circadian clocks are ubiquitous throughout the living world. Of these circadian clocks, the simplest one is found in cyanobacteria - unicellular, photosynthetic marine organisms. Studies of the circadian clock of *Synechococcus Elongatus* PCC 7942 have shown that the circadian clock is independent of genetic transcription and depends only upon the interactions between three proteins - KaiA, KaiB, and KaiC. As such, the cyanobacterial circadian clock provides a unique opportunity to study complex dynamics that can result just from the interactions between three proteins and how the signal from this core oscillator is then subsequently used to drive other mechanisms in the cell.

The purpose of this work was to study the circadian clock *in vivo* to try and understand their interactions in a living cell rather than in a test tube. When the proteins were tagged with yellow fluorescent protein (YFP) and the cells observed with a microscope, a curious phenomenon was observed. The three proteins were found to localize towards one of the poles of the cell when overexpressed. It was found that the localization of KaiA was dependent on the presence of KaiB and KaiC. Furthermore, it was found that the localization of KaiA was dependent on the specific phosphorylation state of KaiC, namely phosphorylation at the Ser431 site. It was found that the localization of KaiB was independent of KaiC or KaiA and that the localization did not show a preference for one of the poles (new vs. old). That the localization of one protein is dependent upon the phosphorylation state of another gives a strong indication that protein localization is a biologically relevant phenomenon - either in the functioning of the clock itself or some action of the clock on other systems.

Experiments were carried out to investigate whether there was any time-dependent behaviour of localization during the circadian cycle but no such behaviour was ascertained. It was also discovered that overexpression of KaiA caused an inhibition of cell division which might be a mechanism by which cyanobacteria use the circadian clock to regulate cell division.

Thesis supervisor: Alexander van Oudenaarden
Title: Associate Professor of Physics

Acknowledgements

This project was done in partnership with Guogang Dong, from Texas Agriculture and Marine University, who constructed many of the strains that were used in this project without which this project would not have been possible. Bioluminescence measurements on these strains were also performed at Texas A&M by him. I would also like to thank Qiong Yang and Miaoqing Fang for their assistance in the later stages of the project, Carlos Gomez-Urbe for his assistance in image processing, and Jeffrey Chabot for providing very useful information on growing cyanobacteria in his thesis as well as being of assistance when I had questions. Most importantly, I would like to thank Prof. Alexander van Oudenaarden for his continued support in all areas throughout the duration of this work without which it would not have been possible for the project to get to the stage that it is in now.

Contents

1	The Circadian Clock	15
1.1	History	16
2	Cyanobacteria	19
2.1	The key components of the cyanobacterial circadian clock	22
2.1.1	KaiA	23
2.1.2	KaiC	24
2.1.3	KaiB	25
2.2	Protein Complexes Involving KaiA, KaiB, and KaiC	25
2.3	Basic Schematic for a Protein-Based Oscillator	25
3	Observation of Localization of Kai Proteins	29
3.1	Could Polar Localization Play a Role in Circadian Rhythms	30
4	Growing and Preserving Cyanobacteria	31
4.1	Selection with antibiotics	34
4.2	Solid Media	34
4.3	Freezing and Thawing	35
4.4	Transformation Protocol	35
4.5	Time-Lapse	37
4.6	Step-by-step method for preparing the perfusion chamber	38
4.7	Preparing a Sample for Time-lapse	40
4.8	Running the Time-lapse	40
4.9	Time Point Measurements	41
4.9.1	Description of parts	43
5	Quantification of Localization	45
5.1	A Brief Foray Into Image Processing	45
5.1.1	Thresholding	46
5.1.2	Noise Reduction	46
5.1.3	Fourier Transform	48
5.1.4	Morphological Operations	51
5.2	Measuring Localization	55
6	Results	61
6.1	Overexpressed KaiA localizes to the cell pole in a KaiB and KaiC dependent manner	62
6.2	KaiB localizes to the cell pole in a manner that is independent of KaiC and shows no polar preference	62
6.3	The localization of KaiAYFP depends on the concentration of KaiA	63

6.4	Further evidence that KaiC phosphorylation is required for localization of KaiAYFP	64
6.5	The KaiABC complex as a potential candidate for localization	66
6.6	Experiments to investigate possible oscillations of localization of KaiCYFP	67
6.7	Overexpression of KaiA causes elongation of cells	69
7	Conclusion	75

List of Tables

4.1	The Ingredients of BG-11	31
4.2	Trace Metals Solution	32

List of Figures

2.1	The cyanobacterium prochlorococcus which is thought to be among the early cyanobacteria that evolved to become the chloroplasts in plant cells.(Source: Woods Hole article)	20
2.2	The color of the Red Sea is due to the cyanobacterium Trichodesmium erythraeum which forms filaments(above) composed of many cells containing the red pigment phycoerythrin. These filaments form raft-like colonies that float to the surface of the water giving the sea its characteristic color. (Source: Oceanus magazine, http://oceanusmag.who.edu/v43n2/waterbury.html)	21
2.3	The gene layout of KaiA, KaiB and KaiC	22
2.4	Three dimensional image of KaiC reconstructed using electron microscope images. Source: F. Hayashi et. al., “ATP-induced hexameric ring structure of the circadian clock protein KaiC”, <i>Genes to Cells</i> , 8 , 287-296 (2003).	24
2.5	Possible mechanism for the phosphorylation cycle of KaiC. Source: Y. Kitayama et. al., “KaiB functions as an attenuator of KaiC phosphorylation in the cyanobacterial circadian clock system”, <i>EMBO Journal</i> , 22 , 2127-2134 (2003).	26
2.6	Another possible mechanism for the phosphorylation cycle of KaiC. Source: S. Klodong et. al., “Functioning and robustness of a bacterial circadian clock”, <i>Molecular Systems Biology</i> , 3 , 1-9 (2007).	27
4.1	Schematic for the incubator used to maintain cultures of cyanobacteria.	33
4.2	Method used to prepare the flow cell for time-lapse microscopy.	39
4.3	Microscope setup for time-lapse. Arrows indicate the direction of flow of the medium. Light sources required for the cyanobacteria to grow are not included.	42
4.4	Chambered incubator for entrainment of cyanobacteria.	43
5.1	Sample trans, YFP and rfp images of the strain AMC704-pAM3913.	46
5.2	Conversion of the RFP image into a binary image using three different thresholds.	47
5.3	Pattern of horizontal stripes and its Fourier transform.	50
5.4	Fourier transform subjected to ideal lowpass and its inverse.	51
5.5	Original image and result after removing noise. The difference between the images is quite conspicuous, though not so on paper due to noise generated during printout.	52
5.6	Original binary image and result after dilation with a 5x5 grid.	53
5.7	Original binary image and result after erosion with a 5x5 grid.	54
5.8	The effect of eroding a binary image followed by a dilation of the eroded image using a 5x5 structure element.	54

5.9	The top-hat transform. (a) Original grayscale image showing bright cells on a relatively darker background. (b) Original image eroded with a disc-shaped structure element of radius 25 pixels. (c) Result of dilation of the eroded image using the same structure element. (same as opening the original image). (d) Result obtained by subtracting (c) from (a).	56
5.10	Result after opening the result of the top-hat transform and then applying a threshold.	57
5.11	The phase contrast image before and after overlaying with the segmented image.	57
5.12	YFP image of strain Avo123 showing polar localization of KaiA-YFP.	58
5.13	Idealized curve of cumulative fluorescence against area when progressively thresholding.	59
5.14	Figure showing the results of applying different methods of quantifying localization to Avo123 cells induced with different concentrations of IPTG, measured 24 hours after induction.	60
6.1	Illustration of the induction system in Avo123.	62
6.2	YFP images of strains containing Ptrc:KaiAYFP taken 24 hours after induction with 1mM IPTG. (a) Ptrc:KaiAYFP, WT , (b) Ptrc:KaiAYFP, KaiB null, (c) Ptrc:KaiAYFP, KaiC null. Only (a) which has neither KaiB nor KaiC knocked out, shows localization of KaiAYFP.	62
6.3	Results after inducing Avo121, Avo125 and Avo129 with 1mM IPTG. All three strains show increased localization upon induction.	63
6.4	Localization of strains Avo123 (Ptrc:KaiAYFP, WT) and AMC1548 (Ptrc:KaiAYFP, KaiA null) 24 hours after induction with different concentrations of IPTG. The strain with the endogenous KaiA intact shows greater localization.	64
6.5	Localization of strains Avo123 (Ptrc:KaiAYFP, WT), AMC1548 (Ptrc:KaiAYFP, KaiA null), and AMC1549 (Ptrc:KaiAYFP, Ptrc:KaiC, KaiC null) after induction with 1mM IPTG.	65
6.6	Images taken after induction with 1mM IPTG for strains containing overexpressible KaiAYFP and mutated KaiC. The letters correspond to the specific mutations described in the text.	66
6.7	Localization of AMC1550 (PKaiBC:KaiCYFP) cells as a function of circadian time when grown in LD (Light - Dark) conditions.	68
6.8	Flow cytometry of various strains to investigate oscillation in YFP levels.	68
6.9	Figure showing the fluorescence of four different colonies of AMC704-pAM3913 over a 36 hour period. Each colony is grown from a single cell and the mean fluorescence per pixel of each colony is measured. Times during which some localization was observed within the colony is marked with thicker lines.	69
6.10	Figure showing the fluorescence as measured using flow cytometry for strains AMC1650, AMC1651, and AMC1652 over a course of 24 hours after synchronizing with two LD cycles.	70
6.11	Figure showing the localization of strains AMC1651 and AMC1652 as a function of time when measured over a 24 hour period. Error bars are standard error.	70
6.12	Frames from a time-lapse showing the elongation of Avo123 cells when when grown in medium containing 1mM IPTG.	71
6.13	Images of Avo123 after they have been grown for a week in different concentrations of IPTG.	72
6.14	Mean lengths of Avo123 after they have been grown for a week in different concentrations of IPTG.	72

6.15 Increase in cell length observed for strain AMC1004 after induction with 1mM IPTG.	73
---	----

Chapter 1

The Circadian Clock

Throughout the ages, humans have occupied themselves with keeping track of the passage of time. From the time that he was mentally capable of doing so, man must have noticed that there was a certain periodicity in the events that surrounded him. Daily cycles of light and darkness, the rising and falling of tides, the repeating phases of the moon, the changing of the seasons - all of these seemingly inevitable and eternal cycles no doubt planted the seeds of the thought in his mind that there was indeed a certain order in the chaos that surrounded him, a system of laws that could not be broken and if understood would enable him to anticipate the future. It is no surprise then that throughout history a great deal of intellectual effort has been devoted towards developing time-keeping devices from the sundials that determined the hours to the calendars that determined the years. Powerful systems have been developed to predict the positions of stars in the sky, the exact times of sunrise and sunset, the occurrences of eclipses etc. Today all of us like to carry timepieces with ourselves to help us arrange our daily activities to fit some sort of a regular pattern as we strive to save each passing moment. Most of the things around us, the computer that I am typing this on, the electricity that travels through the mains, the music that is coming through my speakers, all have been designed to follow a particular rhythm. This preoccupation with timing is not just limited to us and our "higher" intellectual capacity, however. In fact almost all organisms of the earth have some system or another, however rudimentary, that they use in order to keep track of time. Specifically, biological systems have evolved methods by which they can in the absence of any external stimulus approximate the twenty-four hour day and night cycle.

The ability to synchronize one's activity to the natural oscillations is highly developed and amazingly accurate in some organisms. In this regard, there are several examples that are worth mentioning [1]. First let us travel to the caribbean, near San Salvador where Christopher Columbus is first thought to have made landfall when he discovered the new world. In this part of the world lives a creature called the Atlantic fireworm which has a curious behavior. As part of the reproduction ritual, groups of females rise to the surface of the ocean and release their eggs, including a discharge of a brightly luminous secretion. The males then "flash like fireflies and rush in to fertilize the eggs." The interesting thing is that this nocturnal firework always occurs at a time centered roughly an hour before moonrise on the night before the fourth quarter of the moon. Now, Columbus himself may have been witness to this display because shortly before he made landfall, he is said to have seen a flickering light which assured him that he was close to it. Many birds have been known to exhibit rhythmic behaviour which can best be exemplified by a quote from the naturalist Frank E. Lutz on the song of the wren: "It is amazingly precise. Morning after morning I heard the song to the minute on the clock, between 5:57 and 5:58 am. This

is indeed a puzzle when you remember that the sun changes its position by four or five minutes every day.” We have just talked about rhythmic behaviour in worms and birds. Moving on to higher animals, it is known that dogs have a sense of time as is demonstrated by farm dogs when they go out punctually to bring livestock back. Even the cows themselves seem to be able to tell the time; as is mentioned in an amusing letter to *Popular Science Monthly* in 1888 in which the author describes how when he was raising cattle, he had developed a habit of feeding the cows salt every Sunday morning. They evidently enjoyed this treat and began to anticipate it; arriving at the milking bars every Sunday of their own accord while on other days they would have to be actively pursued and gathered. If the author forgot the little ration of salt, the cows would patiently wait for an hour or so before moving on to feed. As far the author knew, the cows had no way of telling the days of the week as they were isolated from any other human interaction apart from the author himself. And yet, here they were faithfully counting down the days to the next Sunday, or perhaps salt-day as they might have said amongst themselves. This anecdote is amusing but does raise an important point, i.e., how can we know that the organism is in fact maintaining an internal clock and not just responding to some external time-related cue that may be either natural or man-made? This question becomes increasingly difficult to answer as we investigate organisms with greater awareness of the surroundings and higher mental faculty. The presence of a biological clock is perhaps best investigated in a species where there is limited interaction with the environment that can be well regulated. The simplest of living creatures that we know are plants which have limited interaction with the environment; restricted to light, temperature and nutrient exchange with the soil. But can something as simple as a plant be expected to have an internal clock?

As far as we know, the cycle of day and night has remained 24 hours long for all of the four-billion year history of our planet. As far as the creatures living on its surface are concerned, this cycle is the most dramatic and rapid change in its environment. For twelve hours of the day it is bright and warm, plants can photosynthesize, reptiles can roam about, animals can see. The remaining twelve hours are the exact opposite, cold and dark during which plants shut down their food-making apparatus and animals too look for a safe place to sleep and prepare for a fresh new day. Since the activity of the majority of organisms is limited by the time during which the sun is in the sky, it is advantageous for them to develop some sort of a mechanism using which they can get themselves ready to welcome the arrival of the sun so that no time is wasted in preparation for it. Since life itself began in such an environment, it seems even inevitable that it be the case that organisms, right down to their molecular processes are linked to the day-night cycle. Throughout the entire living history of the earth, no organism has been exempt from this oscillation; for all practical purposes it is eternal, it is so ingrained in us from millennia of evolution that it is only relatively recently that the idea of a relative time has been pondered.

Of all organisms, plants are involved in the most direct interaction with sunlight as it is their only source of food. It is therefore not surprising perhaps, with the benefit of hindsight, that the earliest plants i.e. the cyanobacteria were the first to develop a daily clock. This internal clock is commonly called the “circadian clock” where the word circadian is the combination of two latin words - circa meaning around and dies meaning day. The corresponding approximately 24-hour rhythm is called the circadian rhythm.

1.1 History

It seems natural to assume that people must have had some feeling for the existence of a natural internal timekeeping mechanism for a long time. However, history only remembers

those that document their thoughts and findings. Possibly the earliest documented account of a biological rhythm is due to Aristotle who noted that the ovaries of sea urchins were larger than normal during the time of the full moon. Several other references to biological rhythms can be found in the works of the ancient Greeks. The father of medicine, Hippocrates, urged his students to pay particular attention to the rhythms of body processes in patients, suggesting that an abnormality in bodily rhythm could be a sign of illness. Cicero noticed rhythmic behaviour in oysters. A particularly interesting observation, with regard to the history of the study of circadian rhythms, was made by Androsthene who noticed that the leaves of the tamarind tree opened during the day and closed during the night. This observation is interesting because it directly leads to the first modern observation of a biological rhythm, which was also in plants, but many years were to pass between Androsthene and Mairan. The historical development of the study of biological rhythms presented here has largely been adapted from [1].

The first modern (relatively speaking) recorded observation of rhythmic behaviour in organisms came centuries after Androsthene in 1729 and is attributed to the French astronomer Jean Jaques Ortois de Mairan. In actual fact, the observation was not published by Mairan himself but by his friend Marchant who decided on his behalf that it was worthy of a publication. Mairan, just as Androsthene before him, noticed that a certain plant he owned displayed a daily rhythm in the rise and fall of its leaves. Mairan's new discovery was that when he kept his plant in complete darkness, it still maintained its daily ritual of raising and lowering its leaves. Mairan himself was shy of suggesting that the plant could be keeping track of time using some internal clock but luckily Marchant published the finding noting that the plant opened up its leaves during daytime and closed its leaves during night-time even when it was kept in continuous darkness. As such it is more of an observation rather than a study and we today would readily point out there could be numerous other factors such as temperature, humidity etc. that could have given the plant some cue for its leaves' behaviour. But these were the early days of modern science and we do not even know the species of plant that was observed. In fact the plant classification system would only be published by Linnaeus several years later in 1735. To his credit, Marchant did call upon biologists to investigate the matter further.

The first true study of plant rhythms was carried out by another Frenchman, Henri-Louis Duhamel of the noteworthy title "Inspector of the Academy of Sciences and of the Navy, Member of the Royal Society of London, of the Academies of St. Petersburg, Stockholm, Palermo, and Padua; of the Institute of Bologna, the Royal Society of Edinburgh, of the Societies of Agriculture in Paris and Leyden, and Free Associate of the Royal Society of Medicine," in 1758. He carried out experiments where the plants were carefully kept in total darkness (a leather trunk), and at constant temperature conditions (a wine cave and a hothouse, where the temperature was maintained above normal) and came to the same conclusion as Mairan before him - that the plants were able to continue their daily oscillation in the absence of any external input that he could identify.

The next study of circadian movement in plants would come in the mid 1830's and was due to a Swiss by the name of Augustin Pyramus de Candolle. Instead of observing the movement of plant leaves in darkness, de Candolle went the opposite route. He set up artificial lighting so that the plants he was observing were under constant illumination. As the others before him, he observed that the plants carried on their daily cycles in the absence of external cues. But there was an important difference, the period of oscillation was not 24 hours, it was around 22.5 hours. De Candolle may have therefore been the first to truly measure the circadian period of an organism in the absence of external stimuli. Circadian clocks exhibit their own characteristic time-period which is often slightly different from 24 hours when they are completely isolated from time cues. De Candolle also made another important observation - that if he abruptly changed the time-cycle of

his artificial lighting so that it was now light when the plants were anticipating darkness; after an initial period of “confusion”, the plants would adapt and follow the rhythm of the artificial light source. Thus he successfully identified two of the characteristics that form the modern definition of a circadian clock - a) It must have a free-running period of oscillation of around 24 hours, and b) The clock must be capable of resetting its phase in response to an environmental input. The third characteristic of a circadian clock is that it must be independent of fluctuations in temperature.

There have been numerous other studies on daily plant movements including an important piece of work titled “The power of movement in plants” by Charles Darwin himself. But now we are entering into the 20th century and the volume of work done on the subject of plant movements and circadian rhythms in general increases exponentially so that a text on its own would be required to even touch upon the historical sequence of events leading up to the present day. So I shall now jump straight to the tiny protagonists of our main story - the cyanobacteria.

Chapter 2

Cyanobacteria

Cyanobacteria are the oldest known living creatures, which is perhaps the reason why they are also one of the most abundant creatures on our planet. This is good news for us animals because they are photosynthetic organisms which form the bottom of the food chain, absorbing carbon-dioxide and nitrogen to build food and the basic amino acids necessary for life as well as releasing the by-product oxygen, of little use to the bacteria themselves but vital to the survival of all heterotrophic life on earth. In fact, the atmospheric composition that we know today (20% oxygen) is largely due to the work that the cyanobacteria have done during their long existence. Evidence for the existence of cyanobacteria has been found in the form of microfossils that extend as far back as 3.5 billion years [2].

Cyanobacteria occupy the vast expanse of the oceans and freshwater and diligently carry on the task of fixing nitrogen and carrying out photosynthesis that they have for billions of years. During this time they have seen the rise of many higher plants but they have remained just as indispensable. The chloroplasts which are responsible for carrying out photosynthesis in plant cells in fact originate from cyanobacteria, living symbiotically with the host plant cell; similar to how the mitochondrion lives in a cell. The cyanobacterium prochlorococcus is thought to be of the family of the early cyanobacteria which first developed into the chloroplasts of plant cells. This is because the prochlorophytes contain the same light-absorbing pigment that plants do - chlorophyll B. Other cyanobacteria do not.

The term "blue-green algae" is frequently used to refer to cyanobacteria. This is slightly confusing because various definitions of the word "algae" tend to disregard prokaryotes while other definitions use the word to describe any aquatic organism that is capable of photosynthesis. While cyanobacteria certainly live in water and photosynthesize, they are also prokaryotic, having no nucleus and no specific organelle containing the photosynthetic apparatus. Thus they occupy a sort of middle-ground between algae and bacteria. The term "algae" is a broad description that encompasses a variety of organisms, both unicellular and multicellular, whose only common feature is that they are found in water and lack any of the developed features of higher plants such as roots, leaves, etc. As has been pointed out before, all algae too have derived their photosynthetic apparatus ultimately from the cyanobacteria.

The knowledge that cyanobacteria form the bedrock of life on the earth is fairly recent. Although their presence in freshwater was known, they were not thought to be important in marine habitats prior to 1970. It was in the late seventies that scientists at the Massachusetts Institute of Technology and Woods Hole Oceanographic Institute discovered that they were found in great abundance in the oceans. Since then their presence has been

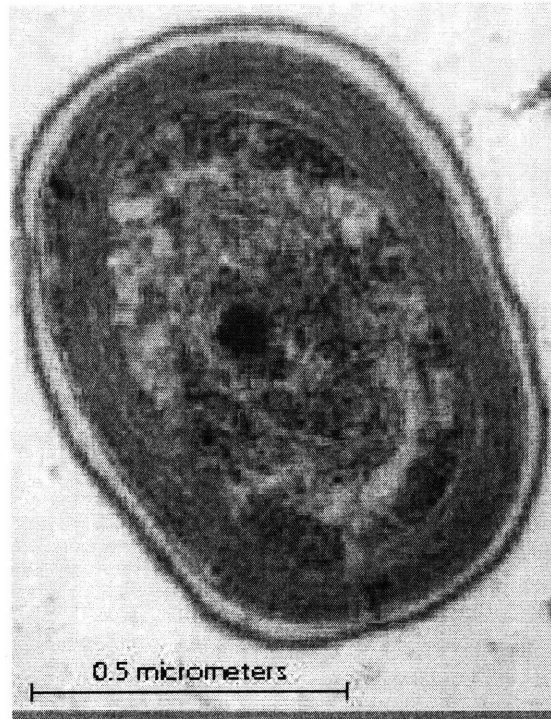


FIG. 2.1: The cyanobacterium prochlorococcus which is thought to be among the early cyanobacteria that evolved to become the chloroplasts in plant cells.(Source: Woods Hole article)

confirmed all over the world's oceans at concentrations ranging from anywhere between a few to more than 500,000 cells per ml. This staggering abundance has established that cyanobacteria are definitely at the bottom of the food chain, fed upon by protozoans, and so on until we eventually arrive at humans. They have been found at any place where there is moisture and light available, and the reader may have encountered them as the green scum that covers the rocks at beaches or more strikingly as the coloration of the Red Sea. So far we have discussed how cyanobacteria make most of the life on earth possible by producing the vast quantities of oxygen necessary for the survival of higher species. They are also equally vital for another extremely important process: nitrogen-fixation.

Nitrogen-fixation is the process in which atmospheric nitrogen is "fixed" or integrated into substances that can be used inside living cells for the manufacture of amino-acids and subsequently proteins. It is thought that the process of nitrogen fixation must have evolved earlier in cyanobacteria than when oxygen was actually present in the earth's atmosphere. This is thought to be the case because the enzyme needed for nitrogen fixation, nitrogenase, is deactivated by oxygen. So the hypothetical chain of events would be that life evolved in an environment where free oxygen was scarce but there was plenty of nitrogen, carbon, water, etc. available. In this environment, the early organisms developed the ability to use gaseous nitrogen to make amino-acids and proteins for self replication. Somewhere along the line, some cells developed the ability to photosynthesize, creating oxygen as a discarded by-product. As these cyanobacteria proliferated, they pumped more and more oxygen into the atmosphere to make up the 20% composition that

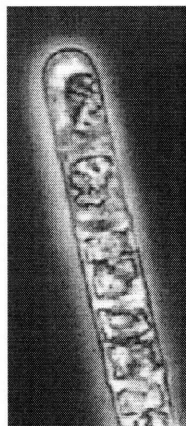


FIG. 2.2: The color of the Red Sea is due to the cyanobacterium *Trichodesmium erythraeum* which forms filaments (above) composed of many cells containing the red pigment phycoerythrin. These filaments form raft-like colonies that float to the surface of the water giving the sea its characteristic color. (Source: Oceanus magazine, <http://oceanusmag.who.edu/v43n2/waterbury.html>)

we know today. The price that they had to pay for this “pollution” was that it led to the evolution of oxygen-consuming species which ate the cyanobacteria for their survival. Many of the cyanobacteria that we know today are capable of both photosynthesis and nitrogen-fixation in the same cell. It has already been pointed out, however that the two processes are incompatible with each other due to the enzyme nitrogenase being deactivated by oxygen. Some cyanobacteria overcome this problem by separating the two processes in time, with photosynthesis occurring during the day and nitrogen-fixation occurring during the night. Other species of cyanobacteria separate the problem in space, with specialized cells in the colonies dedicating themselves to nitrogen fixation while the others are involved only in photosynthesis. In this document, we shall concern ourselves with *Synechococcus elongatus* PCC 7942, a species of cyanobacteria that does not fix nitrogen but still contains a robust circadian clock.

The first evidence that cyanobacteria separate the processes of nitrogen fixation and photosynthesis temporally came around 1986 [3]. In this experiment researchers subjected cyanobacteria to an environment where the light was made to oscillate with twelve hour periods of darkness and brightness. The scientists periodically took samples from the culture and assayed them for oxygen production and nitrogen fixing capacity. It was found that both processes varied from minimum to maximum along with the light dark cycle with oxygen production reaching its minimum in the middle of the night with nitrogen fixation reaching the maximum at the same time. Throughout the experiment, nitrogen fixation and oxygen production were found to be 180° out of phase with each other. What is more interesting in our context is that when the researchers let the light remain on continuously, they found that the oscillations persisted with the same time period. This finding showed that there is an internal mechanism in cyanobacteria which enabled them to keep track of time so as to temporally separate the activities of photosynthesis and nitrogen fixation. Up until this time it had been thought that circadian rhythms were a purely eukaryotic phenomena and it had been assumed that such simple creatures as prokaryotes would not have any need for an internal clock. But the finding of a circadian rhythm in cyanobacteria

indicated that the circadian clock was nearly as old as life itself. It also promised that the mechanism for such a clock could be quite simple as the bacteria themselves are simple organisms. The search for a mechanism for circadian oscillation was on.

In 1993 Susan Golden et. al. used bioluminescence as a reporter to display unequivocally that cyanobacteria had a clear circadian rhythm [4]. They also established the strain PCC 7942 as the lab standard for cyanobacterial circadian clock studies. Serious effort was put into identifying specific genes that were responsible for the circadian oscillations and by 1998 the key players of the system - three genes called KaiA, KaiB and KaiC (from the Japanese word *kaiten* meaning “day”) had been identified. Today we know that a minimal circadian clock can be formed from just these components alone. Several other key genes - specifically SasA and CikA have also been discovered.

2.1 The key components of the cyanobacterial circadian clock

As has just been mentioned, there are three genes that constitute the cyanobacterial circadian clock - KaiA, B, and C. Genetic feedback loops have been known to be capable of producing sustained oscillations in protein levels and therefore such a feedback loop could be a key ingredient in maintaining a circadian oscillation. Recently however, it was shown that oscillations could be achieved *in vitro* using only the three kai proteins in the presence of ATP [8]. This means that protein-protein interactions alone could form the backbone of the circadian clock with the gene feedback loop possibly only serving a secondary purpose of enhancing the effect. Before going on to specifically discuss the proteins themselves, let us take some time to look at the genes responsible for the circadian clock.



FIG. 2.3: The gene layout of KaiA, KaiB and KaiC

The three kai genes are present at the kai locus of the cyanobacterial genome. The KaiA gene is driven by the PKaiA promoter while KaiB and KaiC are bicistronic, driven by the single PKaiBC promoter. Therefore both KaiB and KaiC are encoded as one mRNA but then translated into the two proteins separately. The PKaiBC promoter is fairly strong in cyanobacteria while the transcription of KaiA occurs at roughly one-tenth of the rate of the KaiBC gene. This weak activity of the KaiA promoter translates to the fact that the concentration of KaiA molecules in the cell is far lower than the concentration of KaiB and KaiC molecules. Densitometric analysis of Western blots revealed that there are roughly 500 molecules in a cell while there are around 20000 molecules of KaiC and about 10000 molecules of KaiB [5]. While the expression level of KaiB and KaiC oscillates along with the circadian rhythm, there is not much oscillation seen in the level of KaiA [6]. It is known that KaiC suppresses its own production whereas KaiA enhances the activity of the KaiBC promoter so it was not unreasonable to suspect that the feedback loops that arise could be responsible for the oscillation. Early models of the cyanobacterial circadian cycle ascribed the oscillatory behaviour to a negative feedback loop consisting of KaiC and the KaiBC promoter, thus constituting a TTO (Transcription-Translation Oscillator) model. Further experiments showed however that it is not a TTO system that is responsible for the robust circadian rhythm of cyanobacteria but protein-protein interaction among the kai proteins.

2.1. THE KEY COMPONENTS OF THE CYANOBACTERIAL CIRCADIAN CLOCK

One of the most important hints that transcription/translation is not the root of the oscillation came from tracking the phosphorylation level of KaiC molecules as a function of time. It was found that even in complete darkness, the phosphorylation level of KaiC oscillated between 20% and 80% of the total amount of KaiC present in the cell while maintaining a 24-hour time period of the oscillation [7]. It is known that cyanobacteria practically shut down during complete darkness and mRNA production reaches very low levels [20]. If a transcription/translation system were responsible for the circadian oscillation, then the oscillations ought to stop when the transcription stops. The presence of oscillations despite the lack of protein production is a strong indicator that a TTO system does not form the core of the oscillator. Clear evidence of oscillations being possible in the absence of transcription/translation came in 2005 when it was shown that oscillations in the phosphorylation level of KaiC could be reproduced *in vitro* using nothing more than KaiA, KaiB, KaiC and ATP [8]. Furthermore, it was also shown that mutations in KaiC have the same effect on the length of the period *in vitro* as they do *in vivo*. It is now believed that the phosphorylation cycle of KaiC, generated by interactions between the Kai proteins, forms the core of the circadian oscillator which then drives through a series of interactions that are not very well known, oscillations of the expression level of the genome. The transcription-translation loop involving the Kai proteins is thought to perform a secondary (amplifying or stabilizing) role in the oscillator system. In order to understand how the phosphorylation level of KaiC oscillates without a TT feedback loop, it is essential to understand the function of the kai proteins.

2.1.1 KaiA

KaiA exists in the cytoplasm as a dimer that has a molecular weight of around 20 kDa. Typical of histidine protein kinases which are found throughout the bacterial world, KaiA consists of two domains: the carboxyl terminal effector domain and the amino terminal receiver domain. In the case of KaiA, however, the amino terminal domain is non-functional i.e. it is unable to accept a phosphate group. However, the amino terminal of KaiA is thought to be able to bind to another molecule which would then affect the functioning of KaiA. For this reason, the amino-terminal domain of KaiA is called a pseudo-receiver domain. It is connected to the carboxyl terminal domain by a coiled linker that is around 50 residues long [9]. The carboxyl terminal contains a catalytic domain and a dimerization domain. The dimerization domain contains a conserved motif called an 'H-box' which contains a histidine residue that is able to be trans-phosphorylated by the catalytic domain. In a KaiA dimer, the catalytic domain of one subunit phosphorylates the H-box of the other subunit [10].

As far as functioning in the cyanobacterial circadian system is concerned, the main role of KaiA seems to be to enhance the autophosphorylation of KaiC. It is found that in the presence of KaiA, the rate of KaiC autophosphorylation increases by 2.5 fold [9]. The exact mechanism by which this enhancement occurs is not yet known. The carboxyl-terminal domain of KaiA which is responsible for this enhancement is largely conserved among the various cyanobacterial species while the amino terminal domain is less conserved. In fact, enhancement of KaiC autophosphorylation is unaffected by the removal of the amino terminal altogether, although it is found that such removal tends to lengthen the period of the oscillations [9]. The pseudo-receiver amino-terminal domain of KaiA is thought to bind to clock-input protein(s) (possibly CikA which is essential for resetting the clock) which would alter its interaction with KaiC and thus the rate of KaiC autophosphorylation. It is thought that binding of CikA to KaiA alters the dimerization angle of the carboxyl terminal domains and affect binding to KaiC. This modulation of the influence of KaiA on KaiC could possibly be a mechanism for resetting the phase of the

circadian clock [11].

2.1.2 KaiC

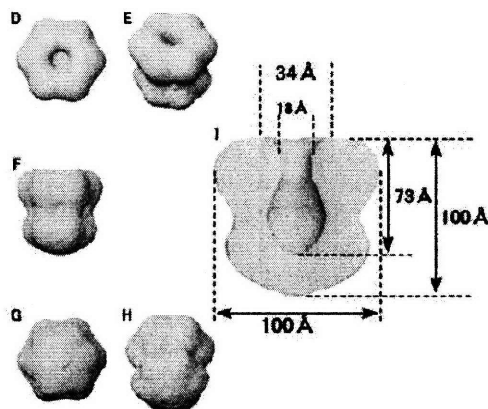


FIG. 2.4: Three dimensional image of KaiC reconstructed using electron microscope images. Source: F. Hayashi et. al., "ATP-induced hexameric ring structure of the circadian clock protein KaiC", *Genes to Cells*, 8, 287-296 (2003).

The next key component of the cyanobacterial circadian oscillator system is the protein KaiC. This protein is encoded by the KaiBC gene, and driven by the KaiBC promoter. The translated mRNA encodes both the KaiC and the KaiB proteins and is subsequently translated into the two proteins. KaiC has autophosphorylation activity which is enhanced in the presence of KaiA.

The monomer of KaiC is a dumbbell shaped molecule. The spherical regions of the dumbbell are thought to correspond to the amino terminal and the carboxyl terminal. In the presence of ATP, it is found that KaiC interacts with ATP and forms hexamers consisting of six monomer units. Each hexamer looks like a hexagonal, pot-shaped structure which is formed by a circular ring of dumbbells lined up side by side. Since there are two phosphorylation sites (Ser-431 and Thr-432) in each monomer of KaiC, there will be 12 total phosphorylation sites in the hexamer [12]. As the KaiC hexamers oscillate between high levels of phosphorylation at dusk and low levels of phosphorylation at dawn, a circadian rhythm is produced. If the KaiC molecules are mutated in a way that prevents their hexamerization, it is found that circadian rhythms are no longer possible, thus KaiC hexamerization is thought to be critical for maintaining circadian rhythms.

It is thought that the ATP-induced hexamerization of KaiC is largely due to the ATP-binding motifs present in the N-terminal domain of KaiC. Each domain of the KaiC monomer is found to contain ATPase motifs (called Walker motifs A and B, or P-loops). Of these, the motifs found in the N-terminal are found to have higher affinity to ATP than the motifs in the C-terminal of KaiC. Further, it is also seen that the N-terminal ATPase motifs are more important for hexamerization of KaiC than the C-terminal motifs [12]. It is thought that while the N-terminal is responsible for binding ATP to form KaiC hexamers, the C-terminal is responsible for binding ATP for the phosphorylation of KaiC.

The phosphorylation reaction consists of the transfer of a phosphate group (specifically the γ phosphate group) from an ATP molecule bound to a C-terminal ATPase motif to one of the two phosphorylation sites of KaiC (also present in the C-terminal).

When KaiA is added to a solution containing KaiC and ATP *in vitro*, the rate of autophosphorylation of KaiC increases by about 2.5 fold [9]. The enhancement of the phosphorylation of KaiC is critical for maintaining circadian oscillations in cyanobacteria which stops in the absence of KaiA.

2.1.3 KaiB

The last ingredient of the oscillator is a protein named KaiB. As explained earlier, it is encoded by the KaiBC gene and driven by the KaiBC promoter. Like KaiA, it exists as a dimer; but unlike KaiA it helps in the dephosphorylation of KaiC rather than its phosphorylation. When KaiA is absent, KaiB is found to have no effect on the phosphorylation levels of KaiC so it is thought that rather than actively dephosphorylating KaiC, KaiB simply opposes the action of KaiA, allowing KaiC to return to its natural rate of autophosphorylation [9]. The exact mechanism by which KaiB achieves this effect is not known. It is also seen that KaiB has some membrane localization which appears to be a function of circadian time. The majority of KaiB is present in the membrane at all times.

2.2 Protein Complexes Involving KaiA, KaiB, and KaiC

The three proteins KaiA, B, and C interact with each other in all possible combinations. We have already discussed the dimerization of KaiA and KaiB as well as the hexamerization of KaiC. Furthermore, the following interactions: KaiA-KaiB, KaiA-KaiC, KaiB-KaiC, and KaiA-KaiB-KaiC are also known to exist. Of these interactions, KaiA-KaiC and KaiB-KaiC have already been discussed. KaiA-KaiC interaction enhances the autophosphorylation of KaiC and KaiB-KaiC interaction probably serves to negate this effect as it has been found that KaiB-KaiC interaction reaches its peak at the time when KaiC is highly phosphorylated and persists until KaiC is largely unphosphorylated [18]. While it is known that the KaiA-KaiB-KaiC complex peaks at late subjective night (before the sun rises), the biological function of this complex is still a mystery. The KaiA-KaiC complex is seen to maintain a relatively low constant level throughout the circadian cycle while it is known that in the presence of KaiA, the phosphorylation level of KaiC saturates fairly rapidly. This suggests that KaiA phosphorylates KaiC by repeatedly complexing and dissociating with KaiC rather than forming a stable phosphorylating complex. Such repeated action is also necessitated by the fact that while the ratio of KaiA molecules to KaiC molecules in a cell is roughly around 5%, it is sufficient to phosphorylate 80% of the KaiC molecules.

While various estimates of the stoichiometry (relative number of molecules) of the complexes based on estimated weights of gel bands have been made, exact numbers are not yet known. Even less is known of the role that these complexes could play in the functioning of the circadian clock but the presence of these complexes both *in vivo* and *in vitro* suggests that they could be vital to circadian clock function.

2.3 Basic Schematic for a Protein-Based Oscillator

With the three Kai proteins that we have just described, we can construct a rudimentary oscillator that shows cyclical change in the phosphorylation level of KaiC. For the sake of

a fiducial point, suppose that KaiC is minimally phosphorylated at dawn (typically in a cell, this corresponds to about 20% of the KaiC being phosphorylated). KaiA and KaiB are of course present in the cytoplasm. As described earlier, KaiA enhances the autophosphorylation of KaiC so in its presence, the phosphorylation level of KaiC increases until at dusk when KaiC phosphorylation has reached its maximum level (typically 80%). When near-maximum level of KaiC phosphorylation is reached, KaiB starts to bind to KaiC and antagonizes the action of KaiA, suppressing the autophosphorylation enhancement. With KaiA rendered inactive, KaiC starts to dephosphorylate during the night until early morning when it reaches its minimum level of phosphorylation. At that point, KaiB leaves and KaiA is free to enhance KaiC phosphorylation again, repeating the cycle. The sequence of events that I have just described is not a certainty. The actual series of steps that take place during the day/night cycle are as of yet unknown. But it is a reasonable hypothesis and we can treat it as a starting point in our effort to understand the clock mechanism.

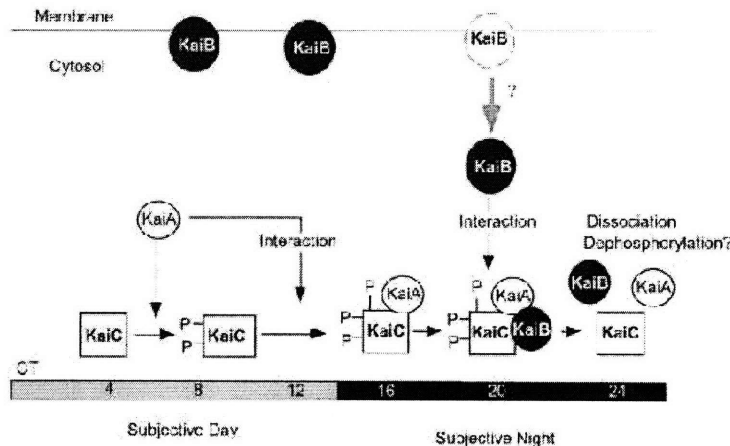


FIG. 2.5: Possible mechanism for the phosphorylation cycle of KaiC. Source: Y. Kitayama et. al., "KaiB functions as an attenuator of KaiC phosphorylation in the cyanobacterial circadian clock system", EMBO Journal, **22**, 2127-2134 (2003).

Although what I have just described could work in principle, a problem arises when one considers the environment in an actual cell. A typical cyanobacterium contains thousands of Kai protein molecules. These molecules will be colliding with each other and with phosphates at random. This would lead to some KaiC molecules having a higher phosphorylation level than others and therefore being at different phases in the cycle. The phase of oscillation of the various molecules would soon be de-synchronized and we would eventually end up with a steady-state system rather than an oscillatory system. In order for the rhythm to persist (as is seen both *in vitro* and *in vivo*) there must be some way in which the phosphorylation level is maintained at nearly equal values for all of the KaiC molecules present. The exact mechanism by which this synchronization is achieved is not yet known but the typical approach that is taken by mathematical models is to allow for rapid monomer exchange among the KaiC hexamers so that on average, all of the KaiC molecules are phosphorylated to the same extent. In order to maintain undamped high-amplitude oscillations, one must also ensure that the actions of KaiA and KaiB are temporally separated so that while phosphorylation takes place during the day,

dephosphorylation takes place during the night only. This is generally achieved by setting up a phosphorylation threshold so that KaiB only associates with KaiC when it has reached a certain level of phosphorylation and persists until another minimum phosphorylation threshold is reached when it dissociates. Depending on the requirements of the model, other features such as sequestration of some protein due to complex formation etc. are added so as to improve the robustness and amplitude of the resulting oscillations. These features are all on display in figure 2.6.

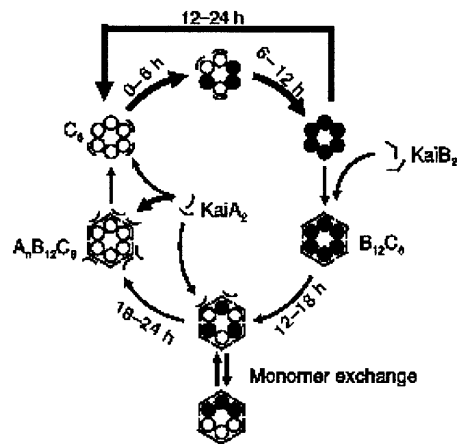


FIG. 2.6: Another possible mechanism for the phosphorylation cycle of KaiC. Source: S. Klodong et. al., “Functioning and robustness of a bacterial circadian clock”, *Molecular Systems Biology*, **3**, 1-9 (2007).

Yet another model discusses the possibility of an oligomeric cluster of KaiC hexamers which would as a whole interact with KaiB so that the phosphorylation level of all the monomers within the cluster would decrease in synchrony [13]. All of the possibilities that I have discussed here are just exercises of the imagination and only experimental evidence will eventually verify which (if any) of these models are representations of the circadian oscillator of cyanobacteria.

Chapter 3

Observation of Localization of Kai Proteins

The fluorescent protein YFP (a yellow variant of GFP) can be used to monitor circadian rhythms in cyanobacteria and was successfully done in [14]. In this construct, a YFPLVA coding sequence driven by the PpsbAI promoter was inserted into the genome of *S. elongatus*. The LVA tag is a sequence of three amino acids, Leucine, Valine, and Alanine which accelerates the degradation of the protein. The gene was inserted into a region called NSI (abbreviation for Neutral Site I), one of the two widely used neutral sites in the chromosome of *S. elongatus*. The psbAI promoter is a strong promoter in cyanobacteria that has been known to follow the circadian clock and bioluminescence experiments used to monitor the cyanobacterial circadian rhythms also typically use this promoter to drive the luxAB gene. The YFPLVA insertion allows the cyanobacteria to produce the yellow fluorescent protein, the rate of production of which depends on the activity of the psbAI promoter. When the promoter is highly active, the cells produce a lot of YFP than when the promoter is less active. Of course there is some time lag between the activity of the promoter and the accumulation of the protein because of delays caused by translation. But apart from the delay, the oscillation in the fluorescence of the cell can be used to monitor the oscillation in the activity of the promoter. This setup allowed Chabot the use of flow cytometry to monitor a large number of cells and show very clearly that the fluorescence oscillated with a 24 hour time period. Under this setup the cells are uniformly fluorescent. A curious behaviour is observed if instead of placing just the YFPLVA gene under the control of the psbAI promoter, the YFP is tagged to the KaiA protein and the resulting KaiAYFP protein overexpressed. For overexpression, the KaiAYFP gene is driven by the Ptrc promoter (forming Ptrc:KaiAYFP) which is a combination of the Plac and the Ptrp promoters and is very highly expressed in cyanobacteria. To complete the induction system, the LacIq gene is also incorporated into the genome (Plac:LacIq). Under normal circumstances, the activity of Ptrc promoter is repressed by the LacIq protein. However, under the addition of IPTG (Isopropyl β - D-1-thiogalactopyranoside), the repression by LacIq is rendered inactive and the Ptrc promoter is free to express the gene under its control. Therefore, the amount of gene expression by Ptrc can be controlled by the amount of IPTG added to the media. When cells containing the induction system just described (Ptrc:KaiAYFP) are induced with any amount of IPTG in excess of 10 μ M, a bright yellow dot is seen to form at one pole of the cell. The nature of this accumulation of KaiAYFP toward one of the poles of the cell is unclear.

An even more interesting behavior is that the polar localization of the KaiAYFP is no longer seen if the KaiC gene is absent. Exactly why this knockout abolishes the polar

localization is unclear as well. In short, we know very little about the structure and the function of the polar localization in KaiAYFP at all.

3.1 Could Polar Localization Play a Role in Circadian Rhythms

An important question to ask is whether or not the observed polar localization is important in maintaining the circadian rhythm in cyanobacteria. The polar localization could be a manifestation of complex formation between KaiA and KaiC or between KaiA, KaiB and KaiC. This would explain why polar localization is not observed when KaiC is not present. If the localization is important for the maintenance of circadian rhythms then it is likely that the level of localization changes in a circadian fashion just as the level of complex formation between the Kai proteins oscillates in a circadian manner. Ostensibly, one would only have to monitor the KaiAYFP strain over several circadian periods to determine whether or not the localization changes in a periodic way. Unfortunately, localization in this strain is only seen when the fluorescent protein is overexpressed and overexpression of KaiA abolishes circadian rhythmicity in cyanobacteria. The requirement that KaiC be present for localization to occur, however, is strong indication that the polar localization of KaiA is a biologically important phenomenon. If one tags the KaiC protein with YFP, and drives it using the PkaiBC promoter, one can see polar localization as well. This strain, while not perfect, holds more promise for showing circadian rhythms in localization than the KaiA overexpressed strain. Using this strain, we can either observe the cyanobacterial cells using timelapse microscopy or observe many cells at various times through several circadian periods in order to statistically determine whether or not the localization level is changing or not. The investigation of polar localization of the Kai proteins forms the bulk of this work.

Chapter 4

Growing and Preserving Cyanobacteria

In order to grow healthy cultures of cyanobacteria, one has to ensure that they have an adequate supply of various salts that they need, a good light source, and exposure to the atmosphere so that they can absorb carbon dioxide. Since the strain PCC7942 is not capable of fixing nitrogen, nitrogen must be provided in the medium using salt sources. The media used for growing *S. elongatus* is called BG-11. This media can either be purchased in concentrated form from biochemical vendors such as Sigma-Aldrich or can be prepared in the lab using basic chemicals. The recipe for preparing BG-11 is given in table 4.1.

Table 4.1: The Ingredients of BG-11

Ingredient	Concentration
NaNO ₃	1.5 g / L
CaCl ₂ · 2H ₂ O	0.036 g / L
FeNH ₄	0.012 g / L
Disodium EDTA	0.001 g / L
K ₂ HPO ₄	0.04 g / L
MgSO ₄ · 7H ₂ O	0.075 g / L
Na ₂ CO ₃	0.02 g / L
Trace Metals	1 ml / L

The trace metal solution used in preparation of BG-11 contains various metal salts as described in table 4.2.

In order to maintain healthy cultures of cyanobacteria, one must ensure that the cells have an adequate supply of light as well as adequate exposure to air so that they have a supply of carbon dioxide. Cultures that are grown in tubes that are tightly capped but otherwise in ideal conditions lose their coloration over a few days and die. Healthy cultures have a rich grass-green color while unhealthy cultures can be recognized by a pale green or even yellow coloration much like a withering leaf. The optimum temperature for maintaining cultures is 30° C, but cells can grow at temperatures as low as 26° C and even as high as 32° C. Besides temperature and availability of carbon dioxide, the last remaining factor to take care of is light. *S. elongatus* must prepare its own food using sunlight (preferably) and

Table 4.2: Trace Metals Solution

Ingredient	Amount in 1L Water
H_3BO_3	2.86 g
$\text{MnCl}_2 \cdot 4 \text{H}_2\text{O}$	1.81 g
$\text{ZnSO}_4 \cdot 7 \text{H}_2\text{O}$	0.222 g
$\text{Na}_2\text{MoO}_4 \cdot 2 \text{H}_2\text{O}$	0.39 g
$\text{CuSO}_4 \cdot 5 \text{H}_2\text{O}$	0.079 g
$\text{Co}(\text{NO}_3)_2 \cdot 6\text{H}_2\text{O}$	0.049 g

there is no substitute for a good, bright source of light. Chlorophyll happens to be most efficient at certain frequencies of light which typically happens to be in the lower frequency range of the visible spectrum therefore light that is rich in blue does not yield best results. Specialty plant growing lamps (either fluorescent or high intensity discharge) work fine but they tend to be expensive and require additional equipment such as a dedicated power source. In the absence of specialized light sources, normal fluorescent tubes are excellent and healthy cultures can be grown when the plants are given a sufficient supply of such light. Light that has a color temperature of around 3700K (normally marketed as cool white or soft white) was found to be the best among the consumer level fluorescent lamps. According to [15], a light intensity of 4200lux is optimal. While measuring intensities is a good way of ensuring uniformity across experiments, there seems to be considerable leeway in one's choice of light intensities. A typical 15W tube light works quite well when placed at a distance of 6 inches or so. Fluorescent tubes marked as being optimized for plant growth also work well. For some reason, compact fluorescent lamps were found to not be as effective as tube lights for growing the cyanobacteria. The basic rule of thumb is brighter is better as long as the temperature does not become a limiting factor. Maintaining the temperature of the culture at around 30°C while providing a bright source of light can be a little tricky. Using fluorescent as opposed to incandescent lamps can help with this a great deal if the cultures are kept in a closed incubator. In all of the incubators used, a sheet of plexiglass was used to thermally separate the hot air near the light source from the cultures. The temperature can then be maintained by either using heaters or fans connected to a temperature controller or by simply adjusting ventilation so that the temperature is such that it is not detrimental to the cyanobacteria. I prefer the second approach because the passive nature of it ensures that the temperature is always at the set point whereas with an active controller, the temperature typically will oscillate around the set point. Further, a spatial gradient of temperature will almost certainly arise due to the positioning of the heater. This problem can be especially acute if one uses a heater that blows air rather than a passive heater such as heating tape. The primary incubator that I used is simply a wooden box containing rows of fluorescent tubes placed on the floor. The tubes were 18", 15W variety and marketed as "Cool White". Roughly five inches above the bottom surface of the box, a large sheet of plexiglass was horizontally placed, creating a transparent table. Holes were cut on the sides of the box below the level of the plexiglass to allow airflow over the tubes. The tubes containing cultures were placed in wire racks on the plexiglass surface. The box extended roughly 18" above the surface of the plexiglass and the lid was simply a piece of board that was placed on the top of the box. By adjusting the position of the lid, the amount of ventilation could be adjusted. For a fairly large set of lid positions, the temperature at the table surface was found to hover somewhere between 29°C and 30°C. The light intensity was roughly 4200

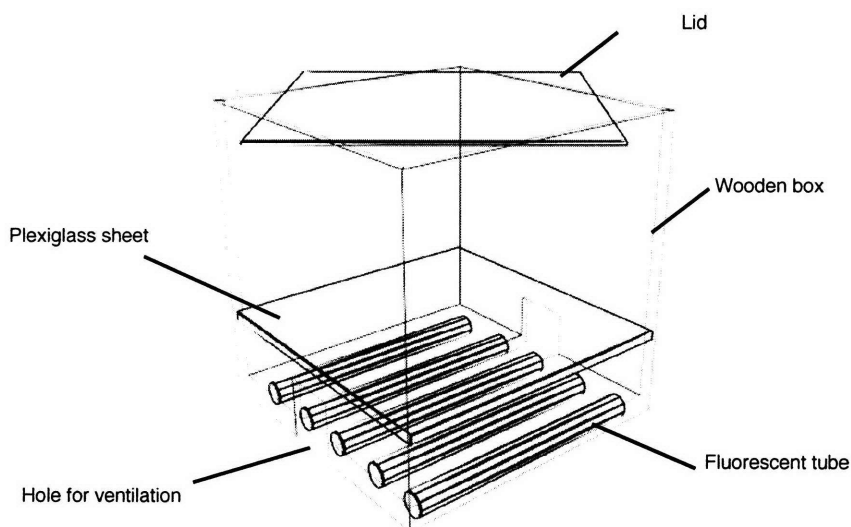


FIG. 4.1: Schematic for the incubator used to maintain cultures of cyanobacteria.

lux. A schematic for this incubator is shown in figure 4.1.

For the culture tubes, BD falcon 50ml tubes were used. Typically, cultures were grown in 10 ml of BG-11 media prepared as described earlier. Various ways of providing access to air are possible. If uniformity across tubes is of particular concern, then one may drill holes in the caps of the falcon tubes and glue a syringe filter to the hole as described in Chabot's thesis. One can then tightly close the cap of the falcon tube. The syringe filter allows for gas exchange through diffusion while foreign particles and microbes are kept out. Further, since all syringe filters are identical, the gas exchange is will be more or less uniform across the tubes. If one need not ensure uniformity to such extent, then it is okay to simply leave the caps loose. Cultures for this work were grown in tubes with caps loose. When growing cultures, it is important to add the appropriate antibiotics to the tube in order to avoid contamination by foreign germs or to prevent proliferation of unwanted variants. When growing several different strains simultaneously, special care must be taken to prevent cross-contamination between the strains as there are typically only two selection antibiotics - spectinomycin and kanamycin used. This means that more than one strain of cyanobacteria will be resistant to a given antibiotic and therefore not selectable. It is wise to try and conduct experiments in such a way that only a few strains need to be grown at any given time. When cultures are thawed for the first time, it takes roughly five days for the tube to develop a green coloration. The culture then grows denser fairly

rapidly after that and depending on the growth conditions as well as the strain being used, will reach a healthy green color in about two weeks. After that, a precipitate of possibly dead cells may be seen at the bottom of the tube and a new culture will need to be started by transferring some of the cells to a new tube. If cultures are kept growing in the same tube for an extended period of time without dilution with fresh media, they will develop a sickly yellow color and if they are not transferred in time, the tube will eventually turn clear with all of the cells sedimented at the bottom of the tube. When transferring a culture to a new tube, 9ml of BG-11 was poured into an empty falcon tube and 1ml of the culture was pipetted into it. An amount of antibiotic appropriate for 9 ml culture, described in the following section, was then pipetted into the tube.

4.1 Selection with antibiotics

All of the strains used in the experiments here had either resistance to spectinomycin or to both spectinomycin and kanamycin. For strains that had resistance to spectinomycin, a stock solution of spectinomycin at 40mg spectinomycin base per ml water was prepared and 5 μ l of this stock solution was used per 10 ml of culture. This amount of antibiotic was lethal to non-resistant strains of *S.elongatus* but did not have detrimental impact on the growth of resistant strains. For strains that were resistant to both spectinomycin and kanamycin, a stock solution of kanamycin sulfate was prepared at a concentration of 50 mg kanamycin sulfate per ml water. 0.5 μ l of this stock solution of kanamycin and 0.5 μ l of the stock solution of spectinomycin as described earlier were then added to 10 ml cultures of doubly resistant strains. The final concentration of antibiotic should be 20 μ g/ml of spectinomycin and 25 μ g/ml of kanamycin for singly resistant strains and 2 μ g/ml spectinomycin and 2.5 μ g/ml kanamycin for doubly resistant strains. The same quantity can also be used for cultures that are transferred from one tube to another.

When cells are thawed for the first time, they should be given some time to grow in antibiotic-free media so that they can build up resistance to the antibiotics. Typically antibiotics were added at least 24 hours after tubes were first inoculated with frozen cultures.

4.2 Solid Media

When carrying out transformations in cyanobacteria, the typical procedure is to plate the transformed cells on selective medium (medium containing antibiotics to which the transformants are resistant) after the transformation and isolate individual colonies that are resistant to the antibiotics. The principle is that each individual colony originated from a single ancestor cell and therefore all of the members of that colony are genetically identical. Transformations are frequently required for experiments and I will describe them here. Since cyanobacteria grow relatively slowly compared to many other unicellular organisms and therefore take time to build up antibiotic resistance, it is important that the petri dish not contain any antibiotics when the cells are first plated. After the cells have been allowed to grow on the antibiotic-free plate for at least 24 hours, the appropriate amount of antibiotic (so that the final concentration is the same concentration as in liquid culture) is pipetted into the petri dish below the agar so that the antibiotic diffuses slowly through the agar and the surface containing the cells does not have an antibiotic concentration that is higher than the full dose. Once single colonies have grown, they can be transferred to a liquid culture or re-streaked on to a fresh agar plate using a sterile pipette tip. Once again, it is better to add antibiotics around 24 hours after the transfer. It takes several days for the liquid culture to show the characteristic greenery of a

growing culture.

In order to prepare agar plates, the BG-11 media must be dissolved in an agarose solution. Typically, a 2% solution of agar (2 grams in 100 ml) is used. Autoclaving BG-11 along with agarose is out of the question because it is possible that heating agarose at high temperatures with the metal ions present in BG-11 can lead to the creation of toxic species. For this reason, a 2X solution of BG-11 is prepared and a 4% solution of agar (Difco agar was used) is prepared separately by autoclaving. The flask containing agar is placed on a stir plate so that the solution is continuously stirred and a thermometer is used to monitor the temperature. When the temperature of the agar solution reaches 55 °C, an equal volume of 2X BG-11 is poured into the flask. The mixture should be stirred until it is homogeneous. The solution is then dispensed into petri dishes (typically 40 ml per plate). The dishes are immediately covered and the agar allowed to solidify. Once solidified, the plates should be stored in a 4° refrigerator. The plates may be individually sealed with parafilm before storage to prevent contamination.

4.3 Freezing and Thawing

Cyanobacteria can be preserved for a long time by storing at -80°C. Since a significant fraction of cells can die due to the stress caused by freezing and thawing, it is important to freeze the cells at high density, but at the same time it is better to freeze the cells that are in the exponential phase than cells that have reached stationary phase. Therefore, in order to freeze cells, they are grown such that the culture is as green as possible without producing any sedimentation. The cells are then centrifuged and the media discarded so as to remove the antibiotics. The cells are then resuspended in 1 ml (or more depending on the size of the pellet) of antibiotic-free media to produce a dense culture. DMSO (dimethyl sulfoxide) is then added to a final concentration of 8% and the liquid is placed in cryo-compatible tubes which can then be placed in the freezer.

When thawing cells that are frozen at -80°C, it is best to use the entire tube. For this reason, it is wise to freeze multiple tubes just in case thawing fails for any one of them. Once the tube has been taken out of the freezer, it is allowed to melt a little bit so that surface of the ice that is contact with the inner walls of the tube has melted. At this point, a sterile wooden applicator is pushed into the center of the tube and the icy block pulled out like a popsicle and dropped into a liquid culture. Typical frozen volumes are 1 ml and therefore the normal procedure is to use 9 ml of BG11 and add the 1ml of frozen culture to it. The culture is then placed in continuous light. Some procedures suggest using cloth screens to shield the culture from full intensity of light as it can be detrimental to the cells when they are first revived but I have always found that cultures can be revived easily at full intensity. As discussed before, antibiotics should be added only 24 hours after the culture is started to prevent a fatal dose.

4.4 Transformation Protocol

Transformation is a process by which new DNA is introduced into the genome of an organism, in our case *S. elongatus*. The two main methods for transforming this species are conjugation and homologous recombination using plasmids. Here I will talk about the second of this two techniques - plasmid transformation. In this method a plasmid (a relatively short, circular piece of DNA) is engineered so that some section of it is homologous to some part of the genome of the cyanobacteria. The homologous part is generally either one of two sites - NSI and NSII (short for neutral site) and the insertion will take place in either one of these two sites depending on which site the plasmid is

homologous to. The plasmid will also contain the gene that one wants inserted into the cyanobacterial genome and some type of antibiotic resistance marker for selection. When the transformation is carried out, the plasmid enters the cell and the genetic machinery of the cell incorporates it into the neutral site that the plasmid was designed for. This incorporation is a random process and only a small fraction of the cells that are subjected to the transformation process will actually incorporate the plasmid into their genome so there needs to be a way of separating the cells that were transformed from the cells that were not transformed. This is where the selection antibiotic comes into play. Once the transformation is complete, the cells are plated on media that contains the antibiotic that the plasmid was designed to provide resistance for. The cells that integrated the plasmid into the genome will survive on the antibiotic plate but cells that were not transformed will die. This way the transformants can be selected and subsequently cultured and stored. The transformation protocol for cyanobacteria is as follows:

- A 10 ml culture of cells is grown to exponential phase.
- The culture is centrifuged and decanted until only 1 ml of concentrated culture remains. This is then transferred to an eppendorf tube.
- The eppendorf tube is centrifuged at 7000 rpm for 3 minutes to create a pellet of cyanobacteria at the bottom of the tube.
- The media is discarded and the cells are resuspended in 1 ml of 10mM NaCl.
- The suspension of cells in NaCl is centrifuged in the same way and the NaCl discarded.
- The cells are resuspended in 600 μ l BG-11. This is divided into two parts of 300 μ l each. One part is used for the transformation while the other part is used for control (one may use as little as 100 μ l for each transformation). Approximately 5 μ l plasmid from a miniprep is added to the suspension that is to be used for transformation. The quantity of plasmid can be increased if the transformation is unsuccessful with this amount.
- The tube is wrapped completely in aluminium foil and placed in a dark chamber at 30°C for at least 8 hours and no more than 16 hours. This step is important because the transformation efficiency in cyanobacteria is greatly increased if photosynthesis is stopped.
- After the incubation, cells are plated on preheated plates (preheated to 30C) and placed in continuous light. The plates are typically 40 ml agar plates.
- Twenty four hours after plating, an appropriate amount of antibiotic should be added to the plates (20 μ g / ml spectinomycin for strains with spectinomycin resistance or 2 μ g /ml spectinomycin and 2.5 μ g /ml kanamycin for strains with both spectinomycin and kanamycin resistance). The antibiotics are typically prepared so that 20 μ l of solution will be required for each plate. It is important that the antibiotic be introduced to the bottom of the petri dish and not to the top in order to avoid a lethal dose of antibiotic to the cells. For this purpose, a spatula is sterilized by exposing it to the flame of a bunsen burner and it is inserted between the agar slab and the wall of the petri dish. The spatula is then drawn all the way around the edge of the agar to loosen the agar slab. It is then inserted below the agar slab so that a side of it is lifted. Care must be taken in this step not to tear the agar. With the spatula holding up the slab, the antibiotic is pipetted into the

bottom of the plate. The spatula is then rotated circularly so that the antibiotic is spread over the bottom of the dish. Despite this, there will inevitably be a concentration gradient of antibiotic across the agar. The spatula is then drawn out and the plate sealed with parafilm to prevent excess evaporation. It can take longer than two weeks for colonies to appear on the plate so preventing evaporation is very important. A small slit is cut in the parafilm to allow for gas exchange.

- Once individual colonies are easily identified, they are extracted using a sterile micropipette tip and immersed into a tube of BG-11 without antibiotics and placed in continuous light. Antibiotics are added 24 hours later.
- Once a healthy culture is growing, the cells should be tested for the desired characteristics and if successful, immediately frozen before any chance of contamination.

4.5 Time-Lapse

Since cyanobacteria are slow-growing organisms and require light and carbon dioxide apart from liquid media, obtaining time-lapse images of growing cyanobacteria presents a significant challenge. The cyanobacteria must be provided with a stable fixed surface for growth so that the cells are maintained in the same position under the microscope objective lens in all three directions of motion - x, y, and z. The best approach is to grow the cells on a small pad of agarose. This semi-solid material traps the cells in a fixed position but still is soft enough to allow for relatively unhindered growth and division of the cells. The most basic problem that arises when doing a timelapse with agar is that during the extended time that the cells must be imaged (on the order of several days), the agar pad tends to dry up unless sealed in an airtight assembly. Sealing, however creates another challenge - hermetic sealing prevents exchange of gases between the agar pad and the atmosphere. In the absence of atmospheric carbon dioxide, the cells will wilt and die. The best approach for ensuring that the cells neither dry up nor are suffocated of carbon dioxide is to keep the agar submerged in media while the time-lapse is performed. Various approaches are possible to ensure to achieve this. The approach used during the course of this work is described here.

A flow cell was created using acrylic slides from Grace Biolabs, a perfusion chamber supplied by Grace Biolabs (part number PC1L - 1.0), a coverslip (24x50mm) and some tubing from McMaster Carr. The perfusion chamber supplied by Grace Biolabs should be 1 mm in thickness for optimal results. If the chamber is too thick, the extended light-path that results makes the images blurry. If the chamber is too thin, it becomes difficult to make an agarose pad of the right size inside it. The perfusion chamber typically consists of a rubber-walled red chamber that is oval internally and rectangular externally. One side of the chamber is covered with a clear plastic surface that is intended for use as a coverslip. Unfortunately, this plastic surface refracts light in unwanted ways which causes the resulting images to be out of focus, therefore the plastic must be removed from the light path in a way that will be described shortly. This plastic surface also contains two holes, one at each end of the chamber meant for pipetting liquids into the chamber. The other side of the chamber is covered with a translucent plastic film that is meant to be removed and the chamber pressed on to a glass slide to create an airtight seal.

To create the flow cell, the first step is to place (not attach) the perfusion chamber on the acrylic slide with the clear plastic surface pressed against the surface of the slide. A marker is then used to mark the position of the holes on the perfusion chamber on the surface of the slide. Holes are then drilled into the position of these holes and tubing

inserted into these holes. The tubing should be roughly 12 inches long for each of these holes. The tubes are sealed in place with epoxy. A reasonable length of tubing (2 mm or so) should be allowed to extend beyond the surface of the slide so that it does not get clogged during the process of epoxying.

Once tubing has been attached to the slide, the next step is to prepare the perfusion chamber itself. A rectangular section should be cut out from the center of the clear plastic side of the perfusion chamber. It is best to carry out this step without removing the translucent film that is on the other side of the chamber. This way, when the film is removed in the final step of the process, a clean surface is presented which will be most likely to create a proper seal. Once the rectangular hole has been cut out, epoxy is applied around the edges of the chamber on the clear plastic surface. The chamber is then placed as before on to the slide (with the clear plastic surface against the slide). If the holes were drilled properly, the tubing should go straight into the chamber. It might be necessary to poke holes into the translucent film to allow the protruding length of tubing to go through. The perfusion chamber should now be pressed against the slide and inspected to make sure that a layer of epoxy has created a good seal all around it. The arrangement should be left to dry for at least an hour after this is complete. This completes the preparation of the perfusion chamber. Step by step instructions for preparing the chamber are given in the following section.

4.6 Step-by-step method for preparing the perfusion chamber

Required Items

- Acrylic slide from Grace Biolabs 1/8" thickness.
- Ordinary glass slide.
- Tubing from SCI (Scientific Commodities Inc.) Internal diameter = 0.72 mm and External diameter = 1.22 mm.
- Epoxy Adhesive.
- Razor Blade.
- Perfusion chamber from Grace Biolabs. Thickness = 1.0 mm.

Method (See figure 4.2)

1. A perfusion chamber and an acrylic slide were taken
2. The perfusion chamber had a thin translucent film covering one of its sides while the other had stiff clear plastic. The clear side also had two holes in it. The translucent film was removed from the perfusion chamber, the chamber was then pressed against the slide and the positions of the holes were marked on the slide using a marker. Using a 1/16" drill bit, holes were drilled into the slide at these positions.
3. The side of the perfusion chamber with the exposed rubber was pressed against an ordinary glass slide. The edges of the chamber were squeezed so that all air pockets between the rubber and the glass were removed and an air-tight seal was formed. Pressing against a glass slide in this manner ensured that the chamber did not get deformed in any way during the epoxying process.
4. Epoxy was applied around the outer edges of the plastic coverslip side of the perfusion chamber and the acrylic slide was placed on to it ensuring that the holes drilled in the slide were aligned with the holes in the plastic of the perfusion chamber. Care was taken

to avoid excess epoxy from making its way towards the center of the slide. Once again, the slide was pressed so that the epoxy was well distributed around the periphery and no air pockets remained ensuring a hermetic seal.

5. The tubing was cut to obtain two pieces, each roughly 18 inches in length. The two pieces of tube were inserted into the holes in the acrylic slide until the tips made contact with the glass slide on the other side. The tubes were then epoxied in place, ensuring that the joints were airtight. The assembly was then allowed to dry overnight.

6. Once the epoxy had dried, the glass slide was removed and using a razor blade, a square region of the clear plastic roughly 1cm X 1cm was cut from the center. This creates a window that allows the most transparent path for light. The raised edges of the cut area also help to hold the agar pad in place and prevent it from sliding when the time-lapse is being taken.

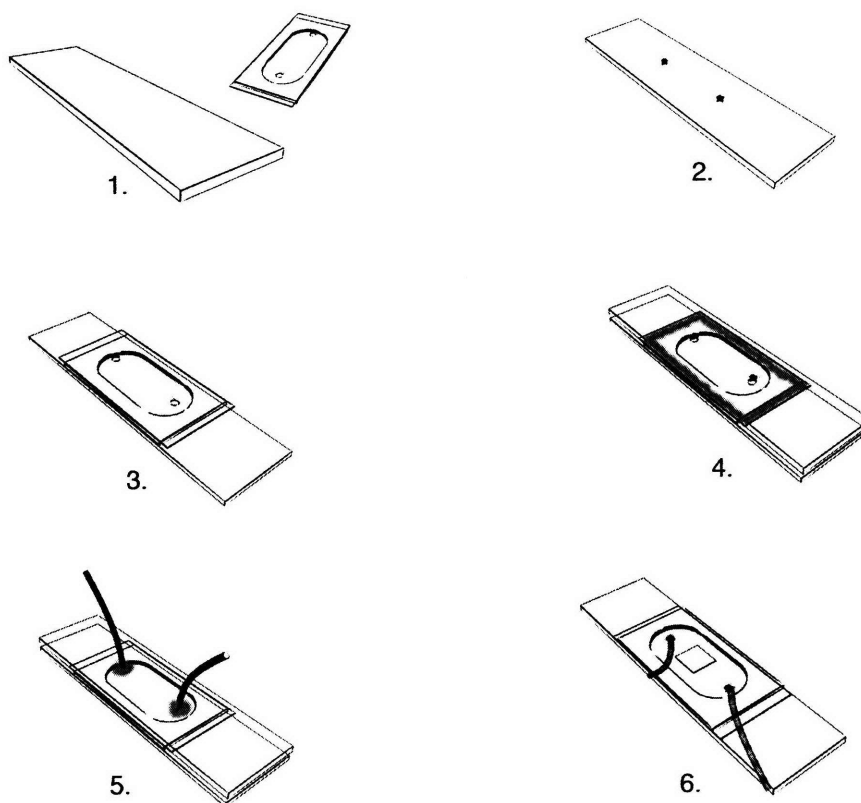


FIG. 4.2: Method used to prepare the flow cell for time-lapse microscopy.

The chamber is then tested to make sure it is airtight by dipping one tube into water while using a syringe to suck from the other ind. If water is successfully drawn into the syringe then the assembly is airtight. The next step is to prepare the sample and the chamber for timelapse.

4.7 Preparing a Sample for Time-lapse

To obtain good results, it is important to make sure that all of the cells being imaged are on the same plane (the bottom surface of the coverslip). To do this, around 150 microliters of the sample to be imaged is placed at the centre of a coverslip of dimensions 24x50 mm. This size of coverslip is ideal for the perfusion chamber, smaller(22x50mm) coverslips are more difficult to deal with. Once the drop of the sample is placed on the coverslip, it should be allowed to stand for around half an hour to 45 minutes to allow the cells to settle and adhere to the coverslip. Since the cells are left in this state for so long, it is best to carry this step out in an environment that has both light and is maintained at a temperature of around 30°C. Therefore, for this purpose, it is useful to have access to a room that is maintained at 30°C.

30 minutes after placing the sample on the coverslip, the agarose media must be prepared. Low melting point agarose is necessary for this because the agar will have to be poured directly onto the cells and regular agar is much too hot when in liquid form to carry out this step. 0.1 g of low melting-point agar is added to 5 ml BG-11 in a plastic tube, boiled in a microwave and then allowed to cool to near 37° C. It is best to use a thermometer for this purpose. Once the agarose media is ready, it should be poured over the cells. First, a micropipette is used to suck all of the drop on the coverslip except for a single liquid layer at the surface (typically this means sucking out as much as possible). Immediately after this, a 125 microliter drop of the agarose media is pipetted onto the cells. The perfusion chamber that was prepared earlier is immediately placed on top of the coverslip and pressed down so that a seal is created between the coverslip and the perfusion chamber. The arrangement is left untouched for a few minutes to allow for the agarose to solidify. After this time, the chamber should be inspected to make sure that a proper seal has formed between the coverslip and the perfusion chamber. If air pockets are seen, gentle pressure is applied to seal the chamber. If it is not possible to seal the chamber at all, one may try to salvage it by applying epoxy around the edges but normally it is best to just start over and create a new one. At the end of the process, one has a perfusion chamber with cells embedded in agarose and two tubes that allow for a flow of media into and out of the chamber. The setup should immediately be placed in continuous light on the microscope stage and media flowed through it.

4.8 Running the Time-lapse

The key to running a successful time-lapse is to ensure that adequate light is available and that the sample is maintained at a temperature of around 30° C. Apart from these requirements, it is also necessary to flow media through the sample to ensure an adequate supply of carbon dioxide and to ensure that the sample does not dry up. Various methods were tried for flowing the media across the sample which can be broadly generalized to gravitational feed and pumping. It was found that pumping was the best approach to use. The main downside to pumping is that the peristaltic pumps used in this study (peristaltic pumps are practical because of the low flow rates possible) do not create a uniform flow. Instead, the pump squeezes liquid through the tube in a very periodic manner. This creates a jerky, pulsatile flow of the media through the flow chamber. This in turn causes either the whole flow cell or just the agarose pad to oscillate along with the flow of the media. Although the oscillation is tiny, the cells are only a few microns long and can be seen to oscillate when viewed through the microscope. This manner of oscillation is unacceptable as stable images cannot be obtained when the object is moving. One way to get around this problem is to use gravitational feed. In this method, the media is placed in a container that is at a higher level than the flow cell and the media is siphoned through

the flow cell into a collection chamber that is placed at a lower level. Once one creates a wick (using tissues, for example) to prevent dripping, this method provides a very uniform flow and eliminates the oscillation of the image. Unfortunately, the pressure inside the chamber is always higher than the pressure outside the chamber in this method which creates a tendency for the liquid to find a way to leak out of the chamber. Since the coverslip interface with the flow chamber is not very carefully sealed using adhesive during the preparation process, a leak almost always occurs.

The best approach was to use a peristaltic pump to suck media through and out of the flow chamber with the media reservoir at the other end. An airtight empty bottle somewhere along the path of the liquid serves to dampen the oscillations of the liquid by maintaining a low pressure environment in the chamber that does not follow the fluctuations of the peristaltic pump. This creates a flow rate that is constant enough that no vibrations of the cells can be seen when observed through the microscope. Liquid that is sucked out of the flow cell is released back into the reservoir to complete the cycle. The source container is open to the air so that gaseous exchange can take place. This way the same media can be recirculated so that no replenishment is necessary during the course of the experiment.

To provide the cells with light, a 30 W fluorescent soft white tubular light source was used. This light source was controlled by a custom-designed relay switch that was controlled by the MetaMorph software used for imaging the cells. The software turned off the lightbulb immediately before an image is taken, fluorescence images are not possible without turning off this bright external source of light. The pump is left continuously on throughout the experiment, even during the image acquisition. If the pump is turned off, a slight change in flow rate or pressure occurs that causes a movement of the agarose pad and sends the cells out of focus. Therefore the best approach is to leave the pump on continuously.

Despite all of this precautions, the agarose pad will show slow and constant movement throughout the experiment and it is necessary to have the software automatically focus the image every three minutes to ensure that the cells are maintained in focus. Since the autofocus algorithm uses only the phase contrast image, it is not necessary to turn the bulb off during focusing. Fluorescence and phase contrast images for storage were taken every 30 minutes during the time-lapse experiments. Some of the experiments were done using a microscope equipped with a laser-based automatic focusing unit. For this system, it was not necessary to focus using the autofocus algorithm.

For maintaining the temperature, a box had been constructed that could enclose the entire microscope. A heater controlled by a temperature controller would maintain the temperature at 30° C. In practice, it was found that the light source alone was sufficient to maintain the temperature at the flow chamber even when the front side of the box was completely open. A brighter light source would necessitate the use of a fan for maintaining the temperature. A diagram of the setup is given in figure 4.3.

4.9 Time Point Measurements

Time-lapse of cyanobacteria is a difficult experiment and the rate of success is quite low. Another way of observing cyclic behaviour is to take periodic measurements through the course of several days. The drawback of this method is that different cells will be used for each measurement and a statistical treatment will be necessary to glean useful information from the measurements. However, with a proper experimental setup, failure of the experiment is unlikely. Obviously it is impractical to take measurements through a time-span of several days so some way needs to be devised such that 24 hours worth of measurements can be taken in a few hours.

For this purpose, a special incubator that contained four chambers was constructed. A

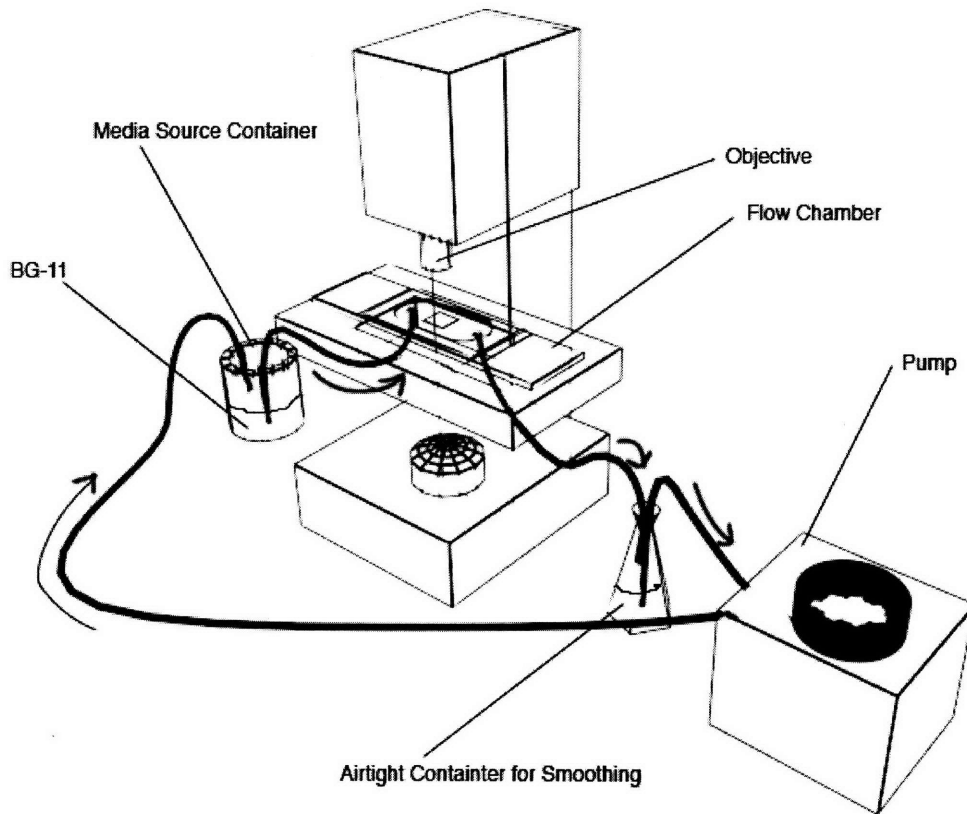


FIG. 4.3: Microscope setup for time-lapse. Arrows indicate the direction of flow of the medium. Light sources required for the cyanobacteria to grow are not included.

separate light source was available for each chamber and the lights were made to come on and off at different times that were six hours apart. This way the cells were entrained to a light-dark cycle that was 24 hours long but each culture was out of phase by six hours from the next. This allowed one to take measurements encompassing all 24 hours within four hours (if measurements two hours apart are taken). Temperature inside the chamber was kept uniform across the chambers using fans that circulated the air around the chambers and the overall temperature was maintained by adjusting the ventilation between the chamber and the air outside. The light sources inside the chamber were sufficient to provide a temperature of around 30 °C without the need of a separate heater. A diagram of the incubator is shown in figure 4.4.

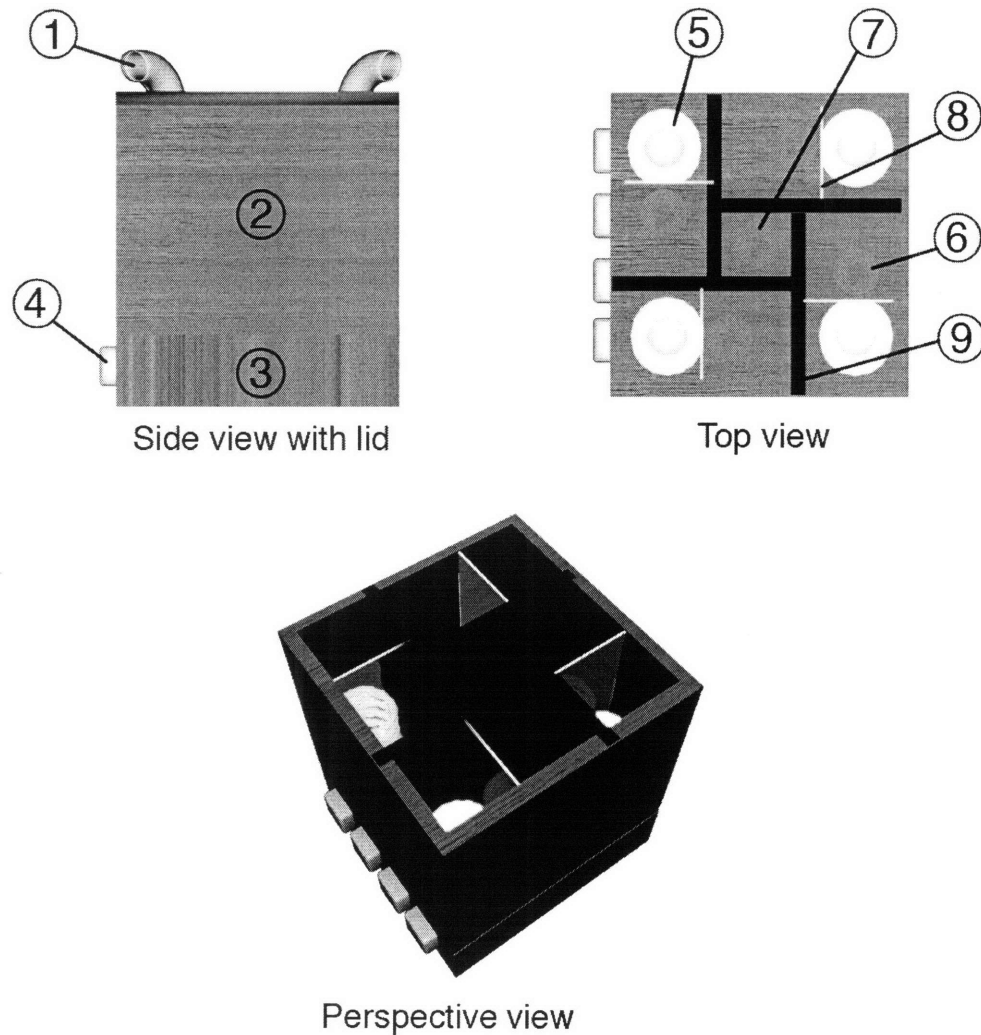


FIG. 4.4: Chambered incubator for entrainment of cyanobacteria.

4.9.1 Description of parts

1. Venting chimney: The chimney serves to remove hot air from the chamber in which the light-bulb is kept so that the temperature in the incubator does not rise above 30° C.
2. Top Chamber: This section of the incubator is divided into four chambers, each of which contains a light bulb for illumination and a fan for air circulation.
3. Bottom Chamber: This is a large hollow chamber. Air from this chamber is blown

into each of the four upper chambers by fans so that the air temperature in all four chambers is the same.

4. Timers: There are four rotary timers that can be adjusted to turn each of the bulbs on and off at desired times.
5. Compact fluorescent bulb: The compact fluorescent bulb is a 3700K 23W bulb from TCP. This bulb provides the light necessary for the cyanobacteria to carry out photosynthesis.
6. Chamber fan: The chamber fan sucks air from the bottom chamber and blows it into the incubation chamber. Constant blowing is necessary in order to ensure that air is well-mixed throughout the four chambers. Since only some of the bulbs are on at any given time, if the air were not blown in this way, chambers with bulbs on would be hotter than the chambers with bulbs off.
7. Central fan: The central fan sucks air from the top of the four chambers simultaneously and blows into the bottom chamber. The air-flow is therefore up from the bottom chamber into the incubation chambers, then into the central chamber and down into the bottom chamber.
8. Plexiglass separator: This plexiglass sheet creates a wall between the bulb and the rest of the chamber. In the absence of this sheet, the temperature in the chamber would rise above 30°. The sheet does not extend all the way down to the bottom of the chamber but stops a couple of inches above the bottom. Air blown into the chamber travels through this gap and cools the bulb as it exits through the chimney.
9. Wall : The wall simply separates the incubation chambers from each other and from the central chamber.

Chapter 5

Quantification of Localization

It is fairly easy to conclude whether YFP is localized or not in a subjective manner but if one wishes to track a trend in localization then it is necessary to develop an objective, quantitative measure of the localization observed in a cell. Since localization by definition entails a non-uniform distribution of YFP fluorescence across the pixels in a cell, it is natural to take some measure of the non-uniformity of pixel intensities as a measure of the localization. However, it is important to have included some spatial information as well because a dozen very bright pixels scattered throughout the cell would in no way constitute the kind of localization that we are seeking. When localization of YFP-tagged proteins occurs in cyanobacteria, it manifests itself as a bright dot located at one of the poles of the cell. The measure of localization was essentially taken to be the ratio of the average intensity of the pixels inside the dot to the average intensity of pixels outside of the dot. Before we can do that however, we must develop computerized algorithms that can differentiate the dot from the rest of the cell and even prior to that differentiate the cells from the background of the image. This is the domain of digital image processing.

5.1 A Brief Foray Into Image Processing

Image processing entails the series of steps from the acquisition of an image to its manipulation so that the final form of the image is ideal for the extraction of the desired information. In our case the task is to simply identify which pixels of an image belong to cells and which pixels belong to the background. This process of identifying relevant parts of an image is known as image segmentation. Image processing methods, collectively known as morphological operations will be used for this purpose. To apply these techniques, we start with three images at our disposal - phase contrast, YFP, and RFP (all taken in rapid succession). The phase contrast images results in dark cells on a light background. The cyanobacteria show very high autofluorescence in RFP so that the RFP images have bright cells on a dark background. Each image is grayscale with pixel intensities ranging from 0 to 65536 (16 bit). The RFP and phase contrast images will be very useful in segmenting the images. After the segmentation is complete, the YFP image can be used to obtain the localization information that we desire.

The morphological operations discussed here are applicable to grayscale images but the discussion presented will concentrate on the manipulation of binary (black and white) images as the processes are easier to describe in that context. Further, the specific MATLAB implementation will be discussed as well. A binary image is simply a black-and-white image, the black pixels have value 0 while the white pixels have value 1. The object of image segmentation is to assign the value 1 to all the wanted or

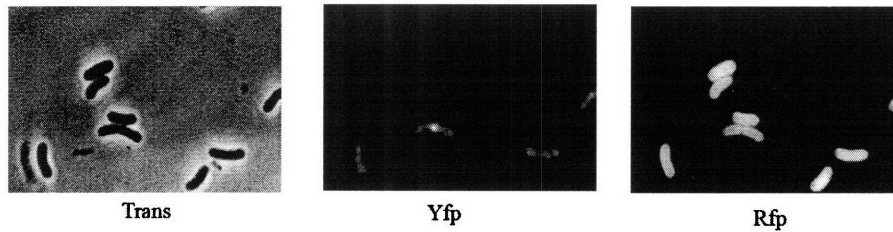


FIG. 5.1: Sample trans, YFP and rfp images of the strain AMC704-pAM3913.

“foreground” pixels and to assign the value 0 to all the unwanted or “background” pixels. Relevant morphological operations are described below.

5.1.1 Thresholding

Thresholding is the process used to convert a grayscale image into a binary image. The procedure is simple. One first determines the appropriate threshold (gray value). All pixels with intensities equal to or higher than this value are assigned the value 1 while all pixels with intensities lower than the threshold value are assigned the value 0. At the end of the operation, one ends up with an image that only has black and white pixels. The choice of threshold completely determines the image that one obtains. A threshold that is too high and a threshold that is too low both could result in a loss of large amounts of detail. As an example, consider the RFP image shown in figure 5.1. As mentioned earlier, cyanobacteria show high autofluorescence in red and in this image we can clearly see bright cells on a dark background which should be ideal candidates for segmentation by thresholding. This is a 16 bit image so the possible range of pixel intensities is 0 through 65536. In this particular image, the lowest intensity is 743 and the highest intensity is 4607 (as determined using MATLAB). Therefore we should use a value somewhere between these extremes as a threshold and hope that all the cell pixels are higher than this value while all the background pixels are lower than this value. Figure 5.2 shows examples of the results obtained using different thresholding values.

In the low threshold image, a threshold value of 900 was chosen. Because of the low threshold, pixels that were actually not within the cell boundary were deemed to be bright enough to be part of the cells. As a result, the size of the cells has been greatly exaggerated. The high threshold image (threshold value 3300) has exactly the opposite problem - pixels that should be within the cell boundary are deemed to be not intense enough to be part of the cell so that the cells are smaller than they should be. The medium threshold image (threshold 2500) achieves the best result.

5.1.2 Noise Reduction

In any kind of signal acquisition, noise is always a problem. Noise is the collective name given to random fluctuations that are seen in the acquired signal that are not due to the behavior of the subject but due to fluctuations in the instrumentation used to collect the signal. The source of these fluctuations can be diverse, thermal fluctuations, electrical fluctuations etc. but the defining property is that they are random, i.e. the fluctuations are as likely to add to the signal as they are to take away from the signal.

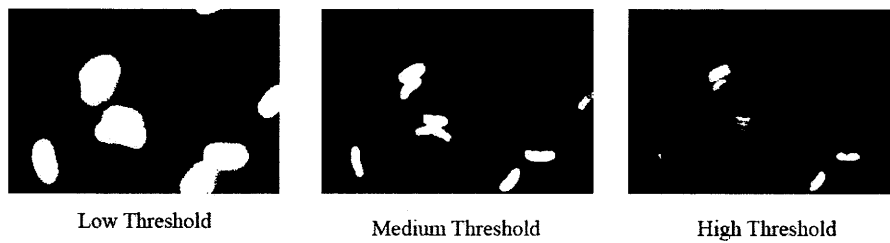


FIG. 5.2: Conversion of the RFP image into a binary image using three different thresholds.

There are many sophisticated algorithms designed to smooth out background noise. Since for our purposes (obtaining mean levels of intensity in a cell, typically) we do not require the extraction of fine detail from noisy data, relatively simple methods of noise reduction will be sufficient. Two of these methods will be discussed here:

1. **Averaging:** The first algorithm that will be discussed here is averaging. As I discussed earlier, random noise is as likely to make the level of the signal be above what it should be as it is to lower the level of the signal. This means that if one takes many samples of the same signal and averages all of the gathered signal, then the random fluctuations will be smoothed out and the actual input signal will dominate.
2. **Lowpass Filtering** If the reader is familiar with electric power supply filtering then lowpass filtering will make sense easily. When designing an electric power supply that is to convert an AC signal to a DC signal, one uses rectifiers (diodes) to convert the AC signal that oscillates both positively and negatively into a rectified signal that still oscillates but only positively, i.e. it never goes negative. This 'bumpy' signal can be thought of as a DC signal of the RMS value combined with an oscillating signal. To turn this into a good, flat DC signal, a lowpass filter (typically simply a capacitor) is used that will 'smooth' out the signal to give a near-constant voltage at the RMS value.

Another widespread and readily understood application of bandpass filtering is the crossover network in loudspeaker systems. The signal output from the audio amplifier is a superposition of signals of all frequencies. Unfortunately, no single loudspeaker is capable of faithfully reproducing the audio at the low frequencies as well as the high frequencies. As a result, a typical loudspeaker system consists of two (or more) drivers. The smaller one is optimized for reproducing high pitched sounds while the larger one is optimized for reproducing the low pitched sounds. To ensure that each speaker receives predominantly the frequencies that it is optimized to reproduce, bandpass filters are employed. A lowpass filter (consisting basically of a capacitor in parallel and an inductor in series) is used with the large driver while a highpass filter (consisting of a series capacitor and a parallel inductor) is used with the small driver.

The principle of signal filtration by suppressing a selected range of frequencies is applicable to image processing as well. In the case of an electronic signal, the signal is a voltage that fluctuates in time. In the case of a digital grayscale image, the signal is a two-dimensional array of values (intensities) in the $x - y$ plane. The principle of filtration by selectively suppressing/enhancing a selected range of frequencies still applies. But first the signal (image) must be represented as a superposition of signals

of different frequencies - this is where the Fourier transform comes in.

5.1.3 Fourier Transform

The Fourier transform is a way of representing a function $f(x)$, as a sum of functions of different frequencies, amplitude and phases. The discrete Fourier transform of a function $f(x)$ is defined as follows.

$$f(x) = \sum_{u=0}^{M-1} F(u)e^{2\pi iux/M} \quad (5.1)$$

The equation above is for a signal that is discretized into M bins so that $f(x)$ is represented by $f(m)$ where $m = 0, 1, 2, 3 \dots M - 1$. The equation tells us that the function $f(x)$ can be represented by a whole bunch of oscillating functions - note that $e^{2\pi iux/M}$ gives us an oscillating function in x for each value of u , the period of which is determined by u according to the formula $\lambda = 1/u$. Since there are M different values of u in the sum, the function f has been represented as a sum of functions having M different periods. The function $F(u)$ assigns a weight to each of these oscillating functions. The function $F(u)$ can itself be complex so the amplitude assigned to each u is actually $|F(u)|$ and the phase is the phase of $F(u)$. In the continuous limit, there is no discretization of the function so the sum is over all possible values of u as follows.

$$f(x) = \int_{-\infty}^{\infty} F(u)e^{2\pi iux} du \quad (5.2)$$

The interesting thing is that the weighing function $F(u)$ itself can be obtained from the original function $f(x)$ by using the following prescription.

$$F(u) = \int_{-\infty}^{\infty} f(x)e^{-2\pi iux} dx \quad (5.3)$$

The function $F(u)$ is called the Fourier transform of the function $f(x)$ and the function $f(x)$ is the inverse Fourier transform of $F(u)$. The functions $f(x)$ and $F(u)$ are said to constitute a Fourier transform pair.

Since our context is image processing, our functions are certainly discrete and therefore we will make exclusive use of equation 5.1. In fact, since the function in this case is two dimensional, we will need to make use of the two dimensional Fourier transform. The translation from one to two dimensions is quite straightforward and the Fourier transform of an image of size $M \times N$ is given by the following equation.

$$F(u, v) = \frac{1}{MN} \sum_{x=0}^{M-1} \sum_{y=0}^{N-1} f(x, y)e^{-2\pi i(\frac{ux}{M} + \frac{vy}{N})} \quad (5.4)$$

The inverse Fourier transform is given by:

$$f(x, y) = \sum_{u=0}^{M-1} \sum_{v=0}^{N-1} F(u, v)e^{2\pi i(\frac{ux}{M} + \frac{vy}{N})} \quad (5.5)$$

In complex notation the Fourier transform, $F(u)$, can be represented as $|F(u)|e^{i\phi(u)}$. The quantity $|F(u)|$ is known as the magnitude or the spectrum of the Fourier transform. The quantity $\phi(u)$ is known as the phase angle or phase spectrum of the Fourier transform.

Note that the Fourier transform of an $M \times N$ image is also a function of the same dimensions but in u, v instead of x, y . The u, v plane is known as the frequency domain as the values of u and v determine the frequency of the component in the spatial domain. It can be shown that the amplitude spectrum of the Fourier transform of a real function is symmetric, i.e. $|F(u, v)| = |F(-u, -v)|$. A minor technical detail is that typically, the function $f(x, y)$ is multiplied by $(-1)^{(x+y)}$ before carrying out the Fourier transform and most packages that support image processing automatically perform this function prior to carrying out the transform. This has the effect of centering the transform at $u = M/2$ and $v = N/2$ rather than at $(0, 0)$ which means that the Fourier transform then appears circularly symmetric about the center of the image that is $M \times N$ in size. When carrying out image filtration in the frequency domain, the procedure is to first compute the Fourier transform of the image and then multiply the transform by a filter function that will selectively boost/suppress a range of frequencies. Then the inverse Fourier transform of the result is computed in order to obtain the modified image.

A simple example of this operation is the notch filter, called so because it affects exactly one frequency component while leaving the others unchanged. Consider for instance the value of the Fourier transform at $(u, v) = (0, 0)$.

$$F(0, 0) = \frac{1}{MN} \sum_{x=0}^{M-1} \sum_{y=0}^{N-1} f(x, y) \quad (5.6)$$

Therefore the value of the Fourier transform at $(0, 0)$ is simply the average intensity of the image. Thus if we wanted the average intensity of an image to change, we could modify the Fourier transform so that $F(0, 0)$ is changed while everything else remains the same. Suppose we have the Fourier transform $F(u, v)$ of an image. We will multiply it with a notch filter $H(u, v)$ which is defined such that $H(u, v) = 0$ if $(u, v) = (0, 0)$ and 1 otherwise. The resulting function $G = FH$ will be identical to F except at $(0, 0)$ where it will be 0. The effect of this filter then is to turn the average intensity of the image to 0 (of course this means that some pixel intensities will have to become negative which is not displayable. The resulting image will need to be scaled so that the most negative value is 0 and all other values are higher.)

The behavior of Fourier transform filters is best understood by using examples. In figure 5.3, we see a pattern of horizontal black stripes on a white background and to the right of it we see the Fourier transform of this image (in u, v space). The Fourier transform contains what appears to be a single vertical white line in the centre of the image. This indicates that waves that oscillate only in the y -direction are required to construct the image (because the actual image only has horizontal stripes). The fact that the white line in the Fourier transform extends all the way across the space indicates that waves of all available frequencies are required. If we look carefully we will notice that the intensity of the white line is not uniform, it is brighter towards the centre and dimmer towards the ends. This indicates that the image is dominated by waves of medium/low frequency. The influence of the various frequencies is best investigated by applying different filters to the Fourier transform.

We shall apply what is called an ideal lowpass filter. The ideal lowpass filter is one which removes all frequencies above a certain threshold while leaving all the lower frequencies untouched. One can think of the ideal lowpass filter as simply a square wave of amplitude 1 centered at the origin. When it multiplies the Fourier transform, all the values close to the origin are untouched while the values farther away are eliminated. Figure 5.4 shows the Fourier transform of the stripe pattern after it has been subjected to ideal lowpass. As we can see, the central white line no longer extends from the top to the bottom of the image but is confined to a narrow region at the center. This tells us that only the low

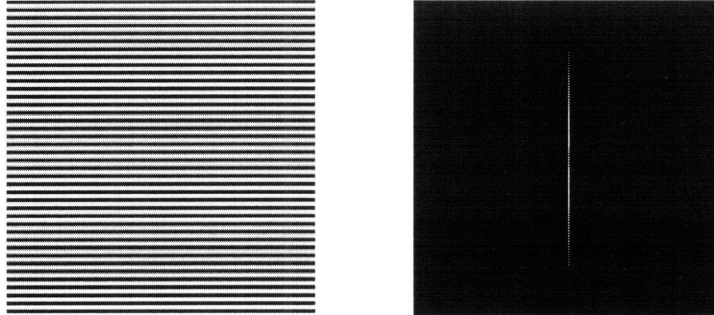


FIG. 5.3: Pattern of horizontal stripes and its Fourier transform.

frequencies will be allowed to exist in the image. The inverse Fourier transform is shown to the right. The final image is grayed, the darks are no longer in sharp contrast to the lights. The effect of the lowpass filter is to ‘smear’ the intensities throughout the image so that all pixels are closer to the average. The general effect of removing high frequency components of any image is to make the image more blurry. A high contrast image has sharp changes in intensity from dark to light regions. This means that high frequency components are required because the intensities need to change by a relatively large amount in little space. If the high frequencies are removed, the intensities will change only over a larger spatial region, resulting in a blurred image.

As we have just seen, lowpass filtering has the effect of removing rapidly fluctuating components of the original image. Noise in an image is also typically of this nature, i.e. it is a rapidly fluctuating component that is superimposed upon the image of interest. Therefore lowpass filtration is a very effective tool for removing noise from an image. The square wave ideal lowpass filter is not the only choice of filter however. One can choose a filter of any shape as long as it suppresses those frequency components that are not desired while boosting those that are desirable. Gaussian filters are a fairly common choice as they have the property of suppressing high frequencies while boosting low ones. The Gaussian filter also has the nice property that the higher frequencies are suppressed gradually rather than having a sharp cutoff like the ideal lowpass filter.

It turns out that a filter function that is very well suited to removing noise is the log-Gabor function. It is defined as follows, where f_0 is the mean frequency, r is the distance from the origin in frequency space and σ is the desired standard deviation of frequency.

$$\text{LogGabor} = e^{-\frac{1}{2} \left(\frac{\ln(r/f_0)}{\ln(\sigma/f_0)} \right)^2} \quad (5.7)$$

By judiciously choosing the values of the mean frequency and standard deviation, one can effectively isolate just the noise components from an image. By subtracting the noise component from the original image, one can then obtain the noise-free image. The procedure goes as follows: One starts off with a filter of low wavelength which isolates predominantly the noise components of the image. Then one progressively employs filters

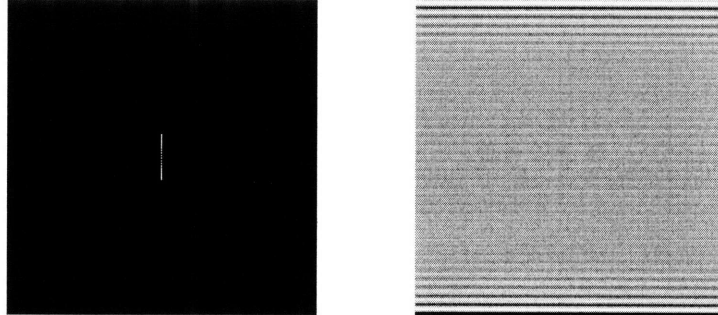


FIG. 5.4: Fourier transform subjected to ideal lowpass and its inverse.

of higher and higher wavelength so that more of the desired components are present with each successive image. The latter images are given high weights while the former images are given low weights. All the images are added up to obtain the final image [16]. The result is illustrated in figure 5.5.

5.1.4 Morphological Operations

Morphological operations are procedures that involve filtering an image using a spatial mask. The best way to describe them is to demonstrate how they work. They are very useful in segmenting images from noisy raw data when simple thresholding will result in a noisy image. In such a situation, morphological operations can help fill in the ‘gaps’ present in the foreground of the image. In the subsequent discussion, the ‘foreground’ pixels will be assumed to be white while the ‘background’ pixels will be assumed to be black. Furthermore, only the application of morphological operations to binary images will be discussed. The principles of application of these operations to grayscale images is similar. Basic morphological operations are described below.

1. **Dilation:** As the name suggests, dilation is an operation that is used to enlarge the size of a foreground object. In its simplest incarnation, dilation can be achieved by simply turning every black pixel that is in contact with a white pixel into a white pixel. This has the effect of drawing a white line around the boundary of the object. A similar effect can be achieved with a spatial mask. In this case a mask (called a structure element) is constructed. A mask is simply a small grid of pixels (not necessarily rectangular) that is used to determine the extent of the dilation process. The mathematical definition of dilation is as follows:

For sets A and B in Z^2 , the dilation of A by B , denoted $A \oplus B$ is defined as:

$$A \oplus B = \{z | (\hat{B})_z \cap A \neq \emptyset\} \quad (5.8)$$

Some set-theoretic definitions are in order. When dealing with images using a set-theoretic notation, it is convenient to think of a binary image as a set of points

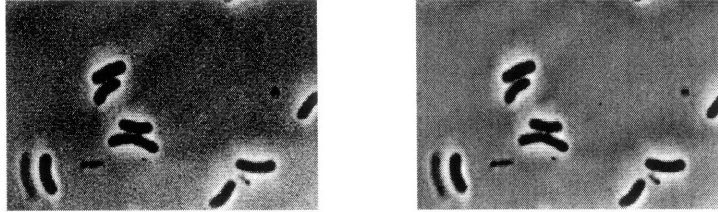


FIG. 5.5: Original image and result after removing noise. The difference between the images is quite conspicuous, though not so on paper due to noise generated during printout.

on a two dimensional plane. This approach is directly applicable to digital images where the image is indeed just a set of pixel co-ordinates that determine the position of the white pixels on a uniformly dark background. Since the pixel coordinates only take on integer values and each point is specified by two numbers (x and y coordinates), a particular pixel is a quantity in Z^2 . The entire image is therefore a set of coordinates in Z^2 .

The reflection of a set B , denoted by \hat{B} , is simply the set obtained by multiplying each coordinate by the minus sign. For example the reflection of $(2, 3)$ is $(-2, -3)$. Therefore \hat{B} is simply B reflected through the origin.

The translation of a set B by the coordinate $z = (z_1, z_2)$ is simply the set obtained when the coordinate z is added to each of the points in the set B . For example the translation of $(2, 3)$ by $(5, 8)$ is $(2 + 5, 3 + 8) = (7, 11)$. The translation of B by z is denoted $(B)_z$.

Let us now revisit equation 5.8 and put it into words: The dilation of the set A by the set B is the set of all points z such that when the reflection of B is translated by z , the intersection of the result with the set A is non-empty. This basically means that the dilation operation selects the coordinates of all the points in the plane that are within 'range' of the points in A , the 'range' being determined by the size and shape of the structure element. Therefore it has the effect of enlarging the boundary of the set A by roughly the size of the structure element. This means that that the definition of dilation can also be written in the following way:

$$A \oplus B = \{z | [(\hat{B})_z \cap A] \neq \emptyset\} \quad (5.9)$$

In practice, dilation is achieved by first choosing a structure element (such as a 3x3 grid, for instance). The centre of the grid is then placed over each of the image pixels in turn. Suppose the grid is placed on the image such that the $(2,3)$ pixel is at the

centre of the grid. If any white pixel of the image falls within the grid of the structure element then the (2,3) pixel in the new image will be white. This procedure is then repeated for all of the pixels in the image in order to obtain the new image.



FIG. 5.6: Original binary image and result after dilation with a 5x5 grid.

As can be seen from figure 5.6, image dilation has two main effects - enlarging the size of the image and filling in gaps present in the image.

2. **Erosion:** Erosion is exactly the opposite of dilation. While dilation enlarges the size of the image, erosion reduces it by turning the white pixels at the boundary of an image into dark pixels. The erosion of an image A by a structure element B is denoted $A \ominus B$ and defined as:

$$A \ominus B = \{z | (B)_z \subset A\} \quad (5.10)$$

In words, the erosion of an image A by a structure element B is the set of all points z such that when B is translated from the origin through z , the points in B fall entirely within the image A . This means that eroding an image picks out those pixels in the image which are a certain number of pixels within the boundary. The number of pixels will be determined by the size and shape of the structure element. The procedure for constructing the eroded image is the same as that for constructing the dilated image except instead of placing the grid on the background pixels and looking for overlap with the foreground pixels, one places the grid on the foreground pixels and looks for overlap with the background pixels. If a background pixel falls within the structure element then the foreground pixel at the centre of the structure element is turned black.

Figure 5.7 shows us the effects of erosion. As described above, erosion makes the features of the image smaller, preserving only those pixels that are in the interior while removing those at the boundary. The major benefit of erosion, however, is that it gets rid of all features that are less than the size of the structure element. The sample image shows a dramatic clean-up of the noisy background after eroding the image.

3. **Opening:** The morphological operation opening is the name given to an erosion followed by a dilation using the same structure element. We just saw how erosion was useful in getting rid of small artifacts from an image with the undesirable side-effect of reducing the size of all the wanted features as well. In order to recover

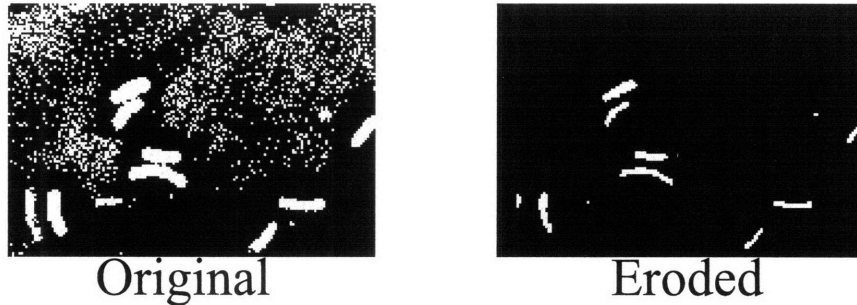


FIG. 5.7: Original binary image and result after erosion with a 5x5 grid.

the original size of the features, we perform a dilation of the eroded image using the same structure element that was used to carry out the erosion. This restores the objects to their original size but as all the artifacts have been lost due to the erosion, the background remains dark.

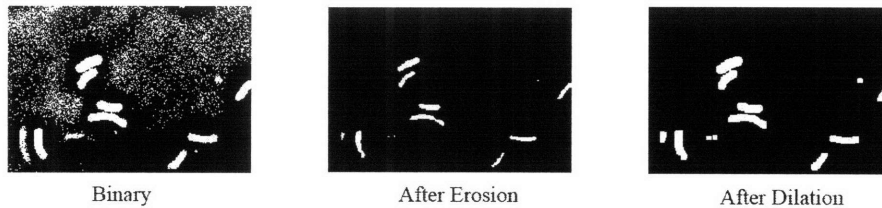


FIG. 5.8: The effect of eroding a binary image followed by a dilation of the eroded image using a 5x5 structure element.

4. **The top-hat transform:** The top-hat transform is the name given to the result obtained by subtracting the result of opening an image from the original image. Since we have only discussed the application of morphological operations to binary images, on first thought it seems that the effect of this would be to remove all the desired features of the image while retaining the background noise. This transform however, is inherently a grayscale transform so a brief discussion of grayscale morphological operations is essential before we can begin to discuss the use of it.

Consider the dilation of a binary image. Here we move the structure element over background pixels and see if any foreground pixels fall within it. If there is a foreground pixel within the structure element, then the central pixel gets turned into the foreground pixel. In a binary image there are only two levels therefore it makes sense to talk of a background and a foreground. In a grayscale image, however, there is no clear boundary between foreground and background. In such a scenario, it is still possible to perform a morphological operation such as dilation. Instead of looking for a 'foreground' pixel, one simply finds the brightest pixel that lies within the structure element and changes the central pixel to that brightness value. The effect of dilation therefore is to make all the pixels around the bright pixel the same

brightness as itself i.e. it makes the local region bright. The effect of a grayscale erosion is exactly the opposite - it makes the local region dark.

Using a grayscale top-hat transform with a structure element that is small compared to the size of the desired features achieves a result similar to applying the transform to a binary image. The opening step gets rid of small artifacts while leaving the large features untouched. Subtracting the opened image from the original image then gets rid of the desired features while preserving small artifacts - exactly what we do not want. The real utility of the top-hat transform is seen when applied with a structure element that is larger than the desired features. Using a top-hat transform on an image that has bright foreground objects on a dark background can very effectively remove artifacts.

As described earlier, the first step of the top hat transform is a morphological opening, i.e. an erosion followed by a dilation. The erosion step turns the local vicinity of a dark pixel to dark - therefore the entire image is turned into a patchwork of dark values. Since the structure element is larger than the size of the bright objects, the bright objects are more or less entirely eliminated from the eroded image. The dilation then further smoothes the patchy eroded image by 'averaging' between the dark patches. The end result of the opening is an image that contains pixels that are of value close to the background pixels but not the absolute darkest pixels present in the image but rather an average among the darkest pixels in the image. When this image is subtracted from the original image, the background becomes more or less uniform and dark (since larger intensities are subtracted from the brighter areas and smaller intensities subtracted from the dimmer areas) while the bright objects in the image still remain brighter than the background by more or less the same amount. An example best clarifies this operation.

Figure 5.9 shows how the top hat transform successfully separates the foreground cells from the background pixels. After the top-hat transform, the bright cells are in stark contrast to the dark background while the original image did not have such a dramatic separation. The final image still shows some noisy artifacts of the background but these are easily removed by opening with a small structure element. The difference between the foreground and background is so stark at this point that a threshold can now be applied to distinguish between the cells and the background. The major utility of the top-hat transform is to make the background uniform so that a threshold can easily be applied.

Once the image has been denoised and subjected to morphological operations for segmentation, we finally obtain the binary segmented image by thresholding. Figures 5.10 and 5.11 show the end result of the segmentation process, where the different colors identify individual cells. Cells that lie at the boundary of the image are ignored.

5.2 Measuring Localization

We now have a way of isolating images of individual cells from the image obtained by using a microscope. The fluorescence image of a cell containing a localized spot of YFP-tagged protein looks like figure 5.12.

In order to measure a trend in the localization behavior, we must first develop a way of quantifying localization in the cells. Several methods of quantifying the localization were investigated. They are described below:

- **Intensity Ratio Using a Fixed Window:** In this method, after the image is

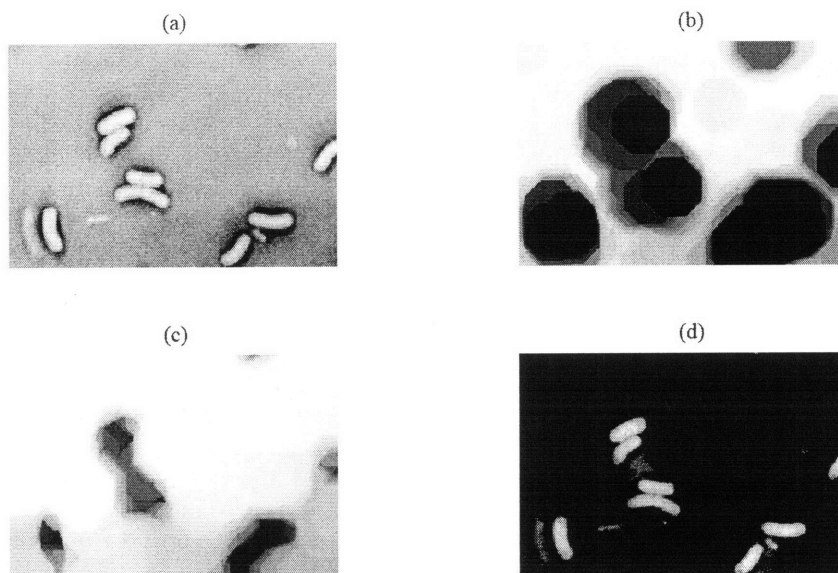


FIG. 5.9: The top-hat transform. (a) Original grayscale image showing bright cells on a relatively darker background. (b) Original image eroded with a disc-shaped structure element of radius 25 pixels. (c) Result of dilation of the eroded image using the same structure element. (same as opening the original image). (d) Result obtained by subtracting (c) from (a).

segmented using the procedure described above, the individual cells are rotated to lie in an approximately horizontal position. Empirically, it was observed that the bright localized spot in the images was typically contained in an area of 3×3 pixels. A search was performed to obtain the brightest 3 pixel by 3 pixel area in the cell. The average intensity of the nine pixels in this window was calculated and compared with the average intensity of the pixels in the rest of the cell. The ratio of the mean intensity inside the window to the mean intensity in the rest of the cell was taken to be the measure of the localization. The higher this ratio, the higher the localization of YFP in the cell.

- Intensity Difference Normalized by Standard Deviation:** This method is essentially the same as the above method, except that instead of taking the ratio between the intensities inside and outside the window, the difference between the mean intensities inside and outside is taken and this quantity is divided by the standard deviation of the the intensities of all the outside pixels. The reason for choosing this method for quantifying localization is to tackle a potential problem with simply taking the ratio of mean intensities. The distribution of pixel intensities in any given cell is unknown. It could turn out that the distribution of the pixel intensities of some cells could have higher variance than the other cells. In this case, just by virtue of the spread being wider, we could get high values of the localization ratio even though the actual intensities might not be very high and we would not consider the YFP to be localized when looking by eye. As an extreme case, consider the uniform distribution in which each pixel intensity has equal probability, i.e. there

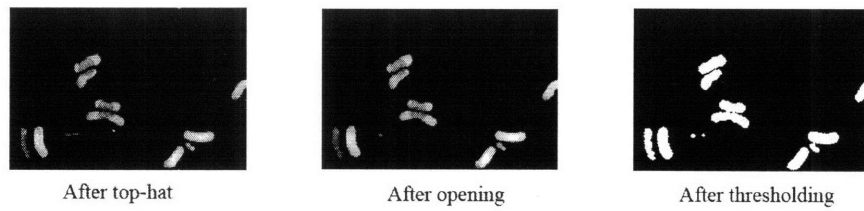


FIG. 5.10: Result after opening the result of the top-hat transform and then applying a threshold.

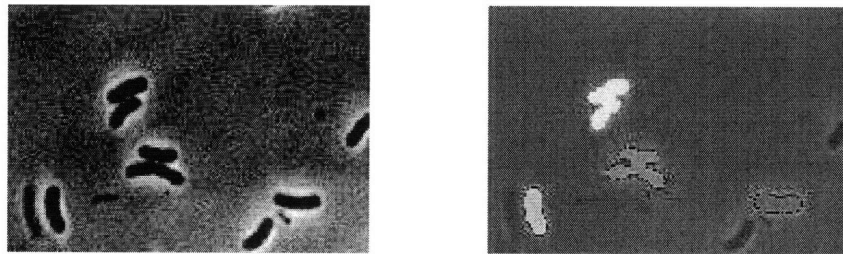


FIG. 5.11: The phase contrast image before and after overlaying with the segmented image.

are the same number of pixels for all pixel intensities within the range of the image. If we lined up these pixels from left to right in a cell, we would get a linear gradient which we would not consider highly localized but would give a high number for the ratio. Normalizing by the standard deviation allows us to compensate for the spread of the distribution by just considering the number of standard deviations away from the mean that the bright spot lies.

- Intensity Ratio Using Curve Fitting to Identify Localization:** Both of the methods described above have the drawback that we use a fixed 3×3 window as the area of the localized spot. However, since the actual size of the spot is not so rigidly fixed, this could lead to an overestimate or an underestimate of the area of the spot. For example, consider the case where the bright spot is larger than the size of the window. In this case, we will overestimate the intensity of the pixels that are not in the bright spot, potentially leading to a smaller value of the intensity ratio than what should be obtained. Similarly, if the size of the spot is smaller than the window then we underestimate the brightness of the spot and again obtain a smaller value of the intensity ratio than we should. Thus it would be useful to have a system by which we can actually identify the size of the spot.

We can get an approximate size of the spot by progressively thresholding the image. First of all, we find the intensity range of the pixels of the image. i.e. the highest brightness and the lowest brightness. Then we start thresholding the image starting

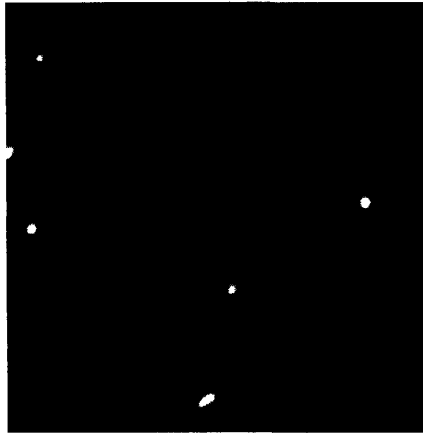


FIG. 5.12: YFP image of strain Avo123 showing polar localization of KaiA-YFP.

at the highest brightest and progressively lowering the threshold by one unit of brightness with each step. At the first step, it is likely that only one bright pixel within the localized spot will be revealed. As we lower the threshold, more and more pixels in the localized spot are going to be revealed. Since the pixels in the spot are very bright, we will obtain high increases of cumulative fluorescence with each increase in area until we start exposing the pixels outside of the spot in which case the increase in cumulative fluorescence will not be as high. If we plot a curve for the cumulative fluorescence of the pixels against the area revealed, it looks like figure 5.13.

In the figure, the total area of the cell is A_2 and the total cumulative fluorescence is F_2 . The slope of the line OB is equal to the average intensity of all of the pixels of the cell. The area A_1 , where the knee of the curve occurs, is the area of the localized spot because the rate of increase of cumulative fluorescence is lower for larger areas. Therefore the quantity F_1/A_1 gives us the mean intensity of the pixels within the localized spot. The mean intensity of the pixels outside of the localized spot is given by the quantity $(F_2 - F_1)/(A_2 - A_1)$. By taking the ratio of these two quantities, we have a measure of the localization in the cell. The main difficulty of this method lies in estimating the location of the knee of the curve. For this, it is useful to use the slope of OB as a reference. On first thought, one may think that the knee probably occurs where the slope of the curve becomes lower than that of OB for the first time. Empirically, it was found that the point where the slope becomes less than 1.5 times the slope of OB gave the best estimate of the knee of the curve.

The above-mentioned method requires that we calculate the slope of the curve at every point. Since the curve is actually a discrete function, the slope fluctuates quite widely and does not give us a nice trend of a high slope to a low slope as we go from left to right along the curve as is the case in the idealized figure. In order to get around this problem, a curve-fit was first applied using the MATLAB function ‘fourier5’ to the discrete curve and the slope of the fitted curve was calculated.

Note that a drawback of this method is that it does not require a point-localization

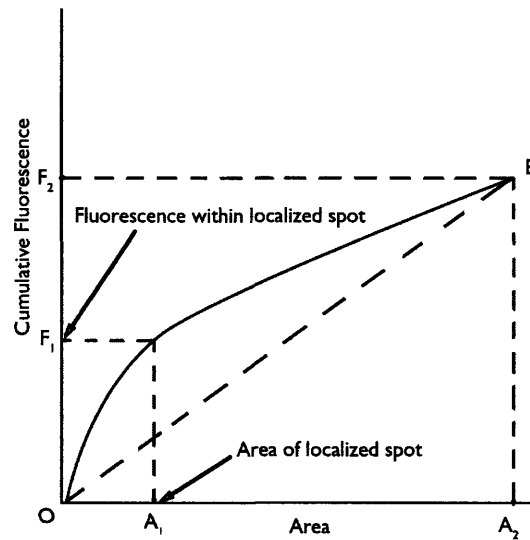


FIG. 5.13: Idealized curve of cumulative fluorescence against area when progressively thresholding.

of the bright pixels at all. We could take all the bright pixels in a cell and scatter them throughout the cell and still get exactly the same curve. In this sense, this method does not really calculate localization in space but localization in intensity only. In practice, however, this was not found to be a problem. Figure 5.14 shows a comparison of all three methods. Note that the localization is seen to decrease at concentrations exceeding $20\mu\text{M}$ IPTG. This is because at such high levels of induction, the size of the localized spot becomes quite large and therefore it is not as localized with respect to the size of the cell. $10\mu\text{M}$ IPTG is sufficient to fully induce this strain to the point of maximum localization (by eye). As we can see, all methods give rise to the same trends. For the analyses of all the data presented in this thesis, the curve-fitting method was chosen.

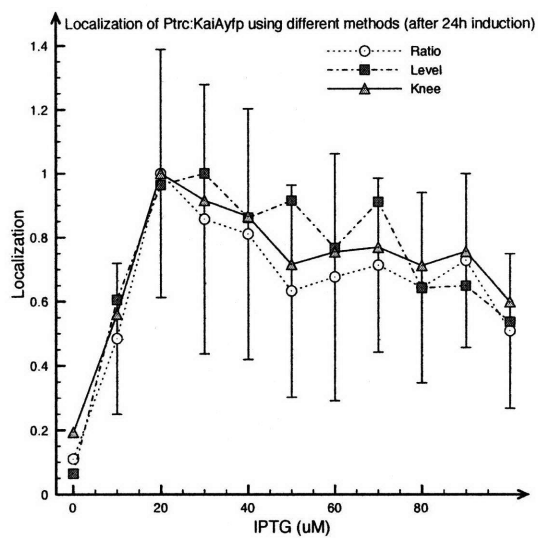


FIG. 5.14: Figure showing the results of applying different methods of quantifying localization to Avo123 cells induced with different concentrations of IPTG, measured 24 hours after induction.

Chapter 6

Results

Many strains were investigated through the course of the experiment. The nature of the various strains will first be described here.

- **PCC 7942:** This is the wild-type laboratory strain of *Synechococcus* that was used for the experiments. All genetic transformations were made on this strain.
- **Avo123:** This strain is PCC 7942 that has been genetically transformed so that it contains a copy of the KaiA-YFP gene. This gene is driven by the P_{trc} promoter which is a strong promoter in cyanobacteria formed by combining regions of the P_{trp} and the P_{lac} promoters. A copy of the lacI_q driven by the P_{lac} promoter is also present. The lacI_q protein normally represses the P_{trc} promoter but upon the addition of isopropyl- β -D-thiogalactopyranoside (IPTG), the suppression is rendered inactive. Therefore the production rate of KaiA-YFP can be controlled by controlling the amount of IPTG added to the medium.
- **AMC1548:** This strain contains P_{trc}:KaiAYFP in a KaiA null background.
- **AMC1549:** This strain contains P_{trc}:KaiAYFP and P_{trc}:KaiC in a KaiC null background.
- **Avo125:** This strain contains P_{trc}:KaiBYFP in a wild-type background.
- **Avo121:** This strain contains P_{trc}:KaiBYFP in a KaiC null background.
- **Avo129:** This strain contains P_{trc}:KaiBYFP in a KaiA null background.
- **AMC1550:** This strain contains PKaiBC: KaiCYFP in a KaiC null background.
- **AMC 704-pAM3913:** This strain contains PKaiBC: KaiCYFP with a 21 amino acid linker between KaiC and YFP.
- **AMC1650, AMC1651, and AMC1652:** These strains are different strains containing PKaiBC:KaiCYFP.
- **AMC1004** This strain contains P_{trc}:KaiA in a KaiA null background.

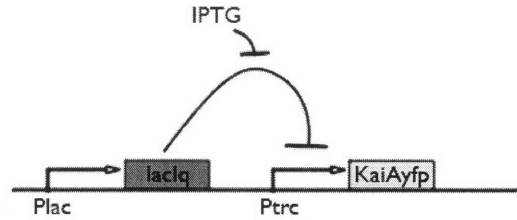


FIG. 6.1: Illustration of the induction system in Avo123.

6.1 Overexpressed KaiA localizes to the cell pole in a KaiB and KaiC dependent manner

When the strain Avo123 is induced with IPTG, it is seen that KaiAYFP localizes at one of the cell poles where it forms a bright dot. However if instead of Avo123, we conduct the same experiment with the strain Avo118 which is also an IPTG inducible KaiAYFP strain but does not contain KaiC, we find that even when KaiAYFP is overexpressed it no longer shows polar localization but is uniformly distributed throughout the cell. Similarly when a strain containing inducible KaiAYFP and KaiC but no KaiB is induced with 1 mM IPTG, the localization is not observed. This is strong evidence to support the claim that the observed localization is not simply aggregation of excess YFP tagged protein but may be biologically relevant. Figure 6.2 shows the results of this experiment.

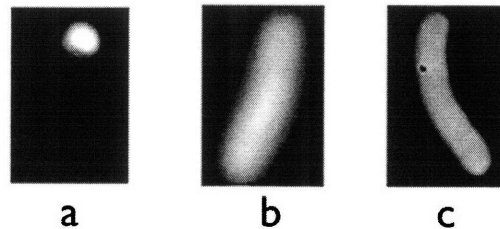


FIG. 6.2: YFP images of strains containing Ptrc:KaiAYFP taken 24 hours after induction with 1mM IPTG. (a) Ptrc:KaiAYFP, WT , (b) Ptrc:KaiAYFP, KaiB null, (c) Ptrc:KaiAYFP, KaiC null. Only (a) which has neither KaiB nor KaiC knocked out, shows localization of KaiAYFP.

6.2 KaiB localizes to the cell pole in a manner that is independent of KaiC and shows no polar preference

The strain Avo125 contains Ptrc:KaiBYFP in a wild type background. When this strain is induced with 1mM IPTG, KaiB is seen to localize at the cell pole. When Avo121, a strain that has the same construct but in a KaiC-null background is induced with the same

amount of IPTG, it is found that the localization of KaiBYFP at the cell pole is maintained. Similarly the strain Avo 129, which contains overexpressible KaiBYFP in a KaiA-null background is induced, localization is seen. This result, shown in figure 6.3, shows that the presence of KaiC or KaiA is not necessary for the localization of KaiBYFP.

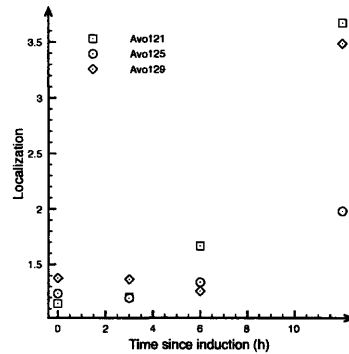


FIG. 6.3: Results after inducing Avo121, Avo125 and Avo129 with 1mM IPTG. All three strains show increased localization upon induction.

Time-lapse experiments (data not shown on paper) in which IPTG was used to induce KaiBYFP and the cells grown under a microscope showed that the localized spots did not show polar preference - i.e. they were just as likely to develop at the new pole after cell division as they were to develop at the old poles.

6.3 The localization of KaiAYFP depends on the concentration of KaiA

Figure 6.4 shows the results of inducing two different strains with increasing concentrations of IPTG. The upper curve is the strain Avo123 which contains P_{trc}:KaiAYFP in a wild type background. When this strain is uninduced, the P_{trc} promoter is mildly active producing a modest amount of KaiAYFP while endogenous KaiA untagged with YFP is also being transcribed. The lower curve is for the strain AMC1548 which contains the same construct as Avo123 except that it is in a KaiA null background. This strain has no endogenous KaiA and all of the KaiA is under the control of the P_{trc} promoter and tagged with YFP. Knowing the nature of these strains, the results of figure 6.4 are surprising because it shows that the presence of untagged KaiA somehow enhances the localization of KaiAYFP. Since the KaiAYFP is driven by the P_{trc} promoter, a promoter which is not natural for cyanobacteria, it is unlikely that KaiA somehow enhances the activity of P_{trc}. If anything, we would expect lower localization for the strain that contains both the KaiAYFP and the untagged KaiA because one could imagine that some of the KaiA involved in the localized dot would be of the untagged variety and would therefore not give any signal.

It is therefore likely that KaiA enhances the activity of some other player which in turn has an effect on enhancing the localization of KaiAYFP. When discussing the nature of the Kai proteins in an earlier chapter, it was mentioned that KaiA enhances the autophosphorylation activity of KaiC. If it were the case that phosphorylated KaiC was

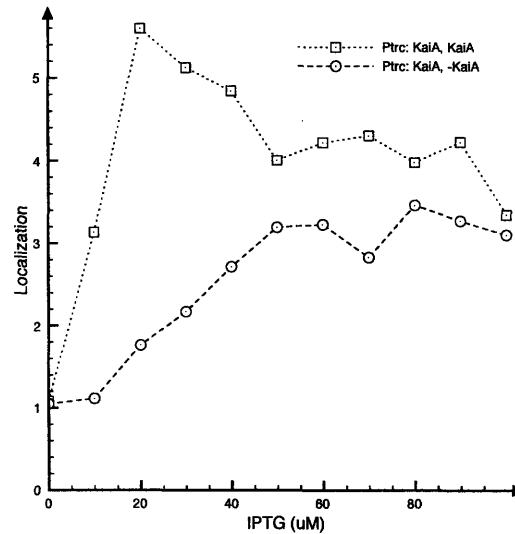


FIG. 6.4: Localization of strains Av0123 (Ptrc:KaiAYFP, WT) and AMC1548 (Ptrc:KaiAYFP, KaiA null) 24 hours after induction with different concentrations of IPTG. The strain with the endogenous KaiA intact shows greater localization.

required for the localization of KaiAYFP then that would explain why untagged KaiA would cause higher localization. A subsequent experiment supports this idea.

6.4 Further evidence that KaiC phosphorylation is required for localization of KaiAYFP

Figure 6.5 shows the results of an experiment in which the strains Av0123, AMC1548, and AMC1549 were all induced with 1mM IPTG and measurements were taken over a 24 hour period to monitor the change in localization of KaiAYFP. The strain Av0123 and AMC1548 have already been described. The strain AMC1549 contains overexpressible KaiAYFP as well as overexpressible KaiC in a KaiC null background. In this strain, both the KaiAYFP and KaiC are simultaneously overexpressed upon the addition of IPTG. We notice in the graph that the strain Av0123 localizes rapidly when induced with IPTG while the remaining two strains localize significantly more slowly. Of the two strains, AMC1549 in which both KaiAYFP and KaiC are simultaneously overexpressed localizes the slowest. This behaviour can be explained by the hypothesis that KaiC phosphorylation is important for localization. In the strain AMC1549 which has co-induced KaiAYFP and KaiC, the addition of IPTG generates excess KaiA but it also generates excess KaiC, thus maintaining the ratio of KaiC to KaiA. On the other hand, in the strain AMC1548 in which only KaiAYFP is overexpressed, there is an excess of KaiA to KaiC which means that AMC1548 should have a higher fraction of phosphorylated KaiC compared to AMC1549 (because KaiA enhances the phosphorylation of KaiC). If the fraction of KaiC that is phosphorylated is important for localization, it would follow that AMC 1549 should localize slower than AMC1548.

One will also notice that at times earlier than 12 hours, the localization of AMC1549 is

higher than the localization of AMC1548. This is most likely because the strain AMC1549 contains endogenous KaiA while the strain AMC1548 does not. It could be the case that at early times, some of the KaiC has already been phosphorylated by the endogenous KaiA and is available for localization.

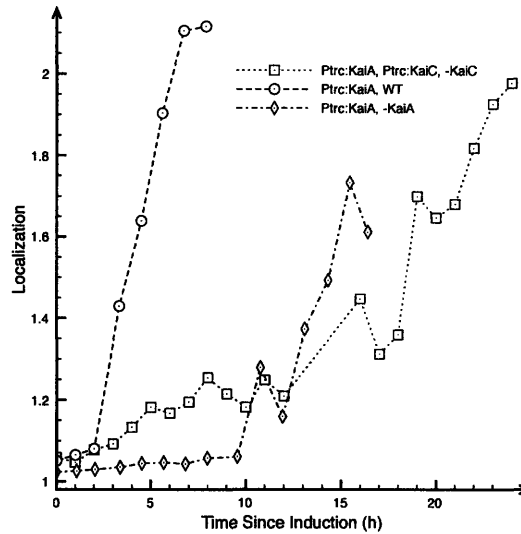


FIG. 6.5: Localization of strains Avo123 (Ptrc:KaiAYFP, WT), AMC1548 (Ptrc:KaiAYFP, KaiA null), and AMC1549 (Ptrc:KaiAYFP, Ptrc:KaiC, KaiC null) after induction with 1mM IPTG.

The most direct evidence for supporting the claim that KaiC phosphorylation is required for the localization of KaiAYFP comes from the construction of KaiC mutant strains. KaiC has two phosphorylation sites - Ser431 and Thr432. By modifying these sites so that they have different phosphorylation states, and transforming the resulting KaiC into a KaiC-null strain containing overexpressible KaiAYFP, we can investigate whether or not KaiC phosphorylation is necessary for localization to be seen. For this purpose, the following modifications to KaiC were made. Each modification of the phosphorylation site changes the phosphorylation behaviour of that site [17].

- (a) KaiC Thr, Ser - Ala : In this mutant, the serine phosphorylation site is replaced by alanine, an unphosphorylatable residue. Thus a strain containing this variety of KaiC will not be able to be phosphorylated at the serine.
- (b) KaiC Thr - Glu, Ser - Ala : This mutant in which the threonine is replaced by glutamic acid mimics a permanent phosphorylation at the threonine site while containing an unphosphorylatable serine site.
- (c) KaiC Thr - Ala, Ser - Asp : This mutant has an unphosphorylatable threonine site while mimicking permanent phosphorylation at the serine site which is replaced by aspartic acid.
- (d) KaiC Thr - Glu, Ser - Asp : This mutant mimics permanent phosphorylation at both the serine and threonine sites.

- (e) KaiC Thr, Ser -Asp : This mutant leaves the threonine site untouched while mimicking permanent phosphorylation at the serine site.
- (f) KaiC Thr - Glu, Ser : This mutant mimics permanent phosphorylation at the threonine site while leaving the serine site untouched.

Figure 6.6 shows the localization behaviour of KaiAYFP in strains that contain the above mutants of KaiC.

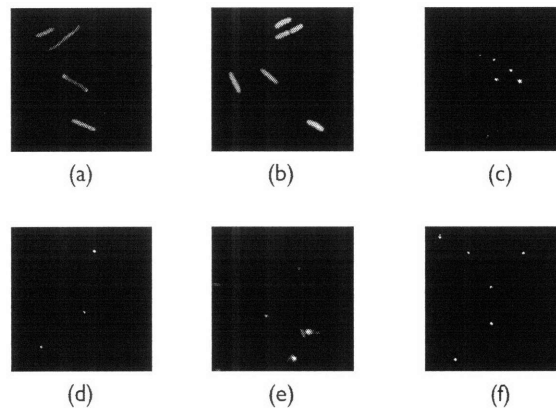


FIG. 6.6: Images taken after induction with 1mM IPTG for strains containing overexpressible KaiAYFP and mutated KaiC. The letters correspond to the specific mutations described in the text.

We can see from the above figure that two kinds of mutations in KaiC abolish the localization phenotype. These mutations are : (a) KaiC Thr, Ser - Ala and (b) KaiC Thr-E, Ser - Ala. In both of these mutations it is the serine phosphorylation site that has been replaced by alanine which is unphosphorylatable. All the remaining mutations have the serine site either unaltered or permanently phosphorylated. Thus we can conclude that it is the phosphorylation state of serine that determines whether or not the cell displays the localization phenotype. Specifically if only the serine is phosphorylated or if both the serine and threonine are phosphorylated then the cell will show localization. However if only the threonine is phosphorylated or if neither site is phosphorylated then the cell will not show localization.

6.5 The KaiABC complex as a potential candidate for localization

Various studies have shown that KaiA, KaiB, and KaiC form a high molecular weight complex during late subjective night, i.e. during the part of the circadian cycle that would normally occur during night time [21] [22]. It has also been discovered that phosphorylation of KaiC at the Ser431 site is necessary for the formation of this complex [19]. These pieces of evidence suggest that the localization of overexpressed KaiA, KaiB and KaiC at the pole of the cell could be a result of this complex. At this point this is merely a hypothesis - there is no reason to suggest why the complex must localize to the

cell pole at all. However, since we know for certain that KaiC phosphorylation is required for localization of KaiAYFP and we know that the phosphorylation of KaiC oscillates with a 24 hour period, we ought to be able to see oscillations in the localization - i.e. it should be possible to see cells with high localization during the part of the circadian cycle where KaiC phosphorylation is high and lower localization when the KaiC phosphorylation. Experimentally it was found that it was not possible to detect such oscillations using KaiAYFP localization. This was because the minimum amount of induction that was required for localization (10 μ M IPTG) was sufficient to abolish the circadian rhythm. The circadian oscillation is dependent on the concentration of the Kai proteins. If there is an excess of KaiA, KaiC becomes hyperphosphorylated and fails to relax back to the unphosphorylated state, causing the circadian oscillations to cease. Further, overexpression of KaiA was also found to disrupt cell division in the cyanobacteria. Since it was impossible to have both the circadian oscillation and KaiA localization simultaneously, it was thought that perhaps it may be possible to monitor potential localization oscillations using KaiCYFP instead. As described earlier, KaiCYFP also shows polar localization but does not need to be overexpressed. Thus if the localization of KaiC coincides with the localization of KaiA then we might be able to see such oscillations using KaiCYFP.

6.6 Experiments to investigate possible oscillations of localization of KaiCYFP

The strain AMC1550 has the construct PKaiBC: KaiCYFP in a KaiC - null background. While the localization of KaiC in this strain is not as sharp as the localization of overexpressed KaiAYFP, this strain shows some localization without the overexpression of any of the Kai proteins.

In order to test whether KaiCYFP showed oscillations in polar localization, the strain AMC1550 (PKaiBC:KaiCYFP, KaiC null) was subjected to both time-lapse and time-point experiments. Unfortunately, bioluminescence experiments showed that the strain was not rhythmic but time-point experiments were carried out anyway to investigate the behaviour of the localization when the cells were driven by day and night cycle. For this experiment, the cells were grown in the four-chambered incubator described in an earlier chapter which enabled measurements taken over a course of four hours to cover the entire 24 hour period (at a time resolution of 2 hours). The results of this experiment are shown in the following figure.

Figure 6.7 shows increased localization during the second half of the circadian cycle but since this strain is not rhythmic to begin with, this experiment does not provide good evidence for an oscillation in localization of KaiCYFP. Another strain, AMC 1549 - pAM3913 was constructed in which the YFP was attached to KaiC using a 21 amino-acid flexible linker with the hope that the flexible linker would rescue rhythmicity. This strain showed sporadic rhythmicity in bioluminescence experiments but weaker localization of KaiCYFP. Specifically, when the bioluminescence of this strain was measured using a 96-well plate, some of the wells showed circadian oscillations while other wells did not show circadian oscillations. The cells were subjected to flow cytometry measurements to see whether the level of KaiCYFP oscillated during a 24 hour period or not. The results of flow cytometry on this strain as well as several other strains is shown in figure 6.8.

Figure 6.8 shows that none of the measured strains except the strain containing the construct PKaiBC: YFPLVA in a WT background oscillate. This strain contains no modification of the Kai proteins but simply contains YFPLVA (a faster degrading variant of YFP) as a reporter of PKaiBC promoter activity. However, none of the strains that have modifications to the Kai proteins showed any oscillations. This could be either

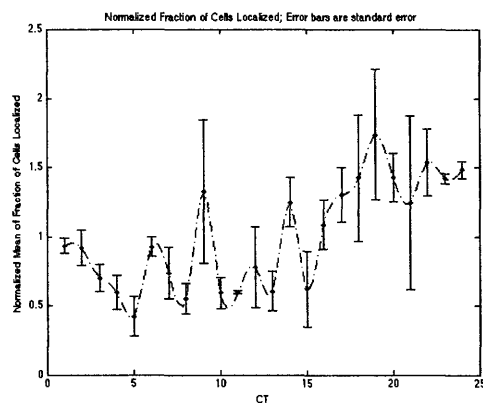


FIG. 6.7: Localization of AMC1550 (PKaiBC:KaiCYFP) cells as a function of circadian time when grown in LD (Light - Dark) conditions.

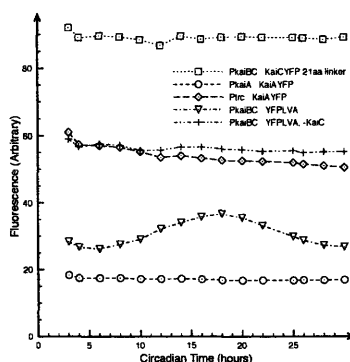


FIG. 6.8: Flow cytometry of various strains to investigate oscillation in YFP levels.

because Kai protein levels do not oscillate, the modifications made to the Kai proteins abolish circadian activity or the cells do oscillate but are somehow out of phase and unable to be synchronized with an external cycle so that the mean total fluorescence level of all the cells remain constant throughout the cycle.

Since the strain AMC704-pAM3913 was found to sporadically show oscillatory behavior in bioluminescence measurements, it was subjected to a time-lapse experiment in order to further investigate its behaviour during a 36 hour period at the single-cell level. The cells were subjected to two LD cycles for synchronization prior to conducting the time-lapse. The result of this experiment is shown in the figure 6.9.

The figure shows that the colonies do in fact oscillate with a near 24 hour period but the colonies are out of phase with each other. This would explain why flow cytometry measurements fail to show any evidence of oscillations. Since each cell is oscillating but out of phase with other cells, the mean measurement of a large number of individual cells will remain constant.

Since the strain AMC1550 was found to be arrhythmic and the strain AMC704-pAM3913

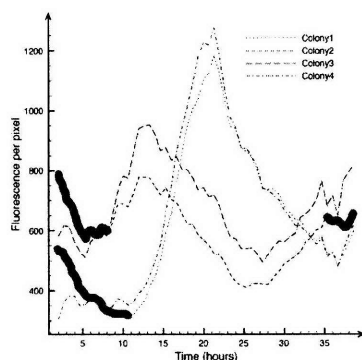


FIG. 6.9: Figure showing the fluorescence of four different colonies of AMC704-pAM3913 over a 36 hour period. Each colony is grown from a single cell and the mean fluorescence per pixel of each colony is measured. Times during which some localization was observed within the colony is marked with thicker lines.

was found to be unsynchronizable, new strains AMC1650, AMC1651 and AMC1652 were constructed. AMC1650 used a variant of YFP called ‘venus’ while the strains AMC1651 and AMC1652 had different linker lengths. Bioluminescence experiments showed that all three strains were rhythmic. It was found that the YFP used in AMC1650 was susceptible to photobleaching and no localization was seen during experiments with this strain. Strains AMC1651 and 1652 showed KaiCYFP localization and therefore promised to be good candidates for investigation of potential oscillatory behavior of localization. Unfortunately, when flow cytometry experiments were carried out, neither strain was seen to show oscillations in the level of fluorescence. Since KaiCYFP is being driven by the PKaiBC promoter which is oscillatory, it was expected that fluorescence of the cells would oscillate. Further, since the strains were found to be rhythmic in bioluminescence experiments, the lack of rhythmicity could not be due to a lack of synchronization. The results of the flow cytometry experiment are shown in figure 6.10.

With the optimistic hope that in spite of no noticeable oscillation in the expression of KaiCYFP, there could still be oscillations in its localization, time-lapse experiments were conducted with the strains AMC1651 and AMC1652. No oscillations in localization were seen. The cells started out showing some localization which slowly dissipated as the time-lapse progressed. The localization did not return even after 36 hours into the time-lapse. Interestingly, movement of the localized spot all the way from one pole to the other and back was seen. To make certain that there was no oscillation in localization, time-points were taken over a 24 hour period. Samples were taken every hour over a 24 hour period, imaged and the images analyzed to find the mean localization of all of the cells at each time point. This experiment did not show any oscillation in localization either. The result of this experiment is shown in figure 6.11.

6.7 Overexpression of KaiA causes elongation of cells

It was discovered that when KaiA is overexpressed in cells, the cell division of *Synechococcus* is harmed. Cells which are grown in the presence of IPTG grow but fail to divide normally. The final equilibrium length that they reach depends on the

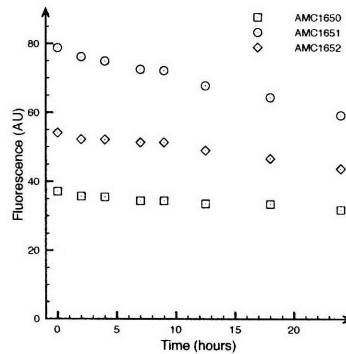


FIG. 6.10: Figure showing the fluorescence as measured using flow cytometry for strains AMC1650, AMC1651, and AMC1652 over a course of 24 hours after synchronizing with two LD cycles.

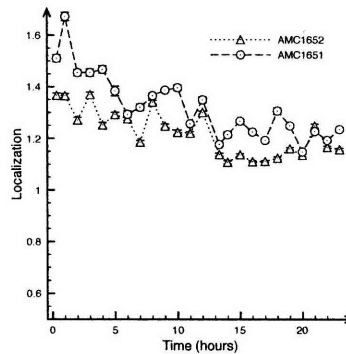


FIG. 6.11: Figure showing the localization of strains AMC1651 and AMC1652 as a function of time when measured over a 24 hour period. Error bars are standard error.

concentration of IPTG that they are exposed to. Figure 6.12 shows frames that have been selected from a time-lapse video of the strain Avol23 that was grown in solid medium containing 1mM IPTG. The goal of the experiment was to observe whether or not there was any change in localization as a function of time. Although a time-dependent variation in localization was not observed, an interesting by-product was the observation of increasing length of the cells. Following this experiment, another experiment was conducted in which cells were grown in varying concentrations of IPTG ranging from 0 to 100 μ M. Sample images of the cells in this experiment are shown in figure 6.13.

In order to quantify the increase in cell length that results from overexpression of KaiA, the length of the cells was measured using image processing software written in MATLAB. The results are shown in figure 6.14. Figure 6.14 shows the lengths increase rapidly at first and then plateau as the concentration of IPTG is increased above 100nM. This behaviour, however is largely due to bias in the measurement process. As the cells become longer, they are less likely to fit in the small window of the camera and therefore the longer cells

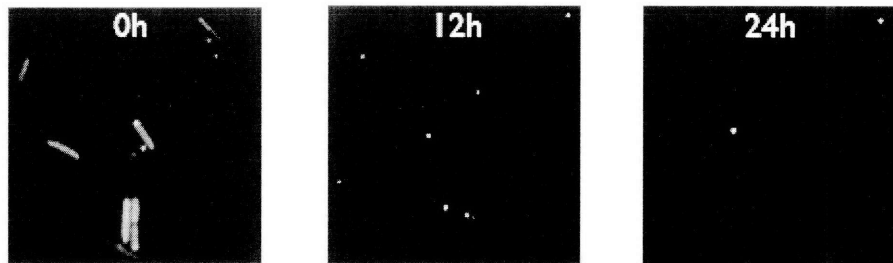


FIG. 6.12: Frames from a time-lapse showing the elongation of Avo123 cells when grown in medium containing 1mM IPTG.

are less likely to get measured. The graph does clearly show that the cell lengths are sensitive to overexpressed KaiA.

One caveat of all the measurements shown above concerning cell length is that in these experiments we are not overexpressing KaiA, but KaiAYFP. It is possible that the effect on cell division is due to the YFP tagged KaiA rather than natural KaiA. Therefore, a strain was constructed in which KaiA, not modified in any way, could be overexpressed using IPTG. This strain was subjected to induction with 1mM IPTG and measurements were taken 48 hours after induction. As a control, the unmodified strain PCC7942 was subjected to the same test. Once again it was found that overexpression causes a clear increase in length leading to the conclusion that overexpression of KaiA causes a malfunction in cell division mechanism of cyanobacteria. The results of this experiment are shown in figure 6.15.

It was also discovered that when the cells that are elongated due to the effect of KaiA overexpression are washed so that they are no longer under induction, they regain their ability to divide. The elongated cells undergo multiple divisions to produce numerous daughter cells.

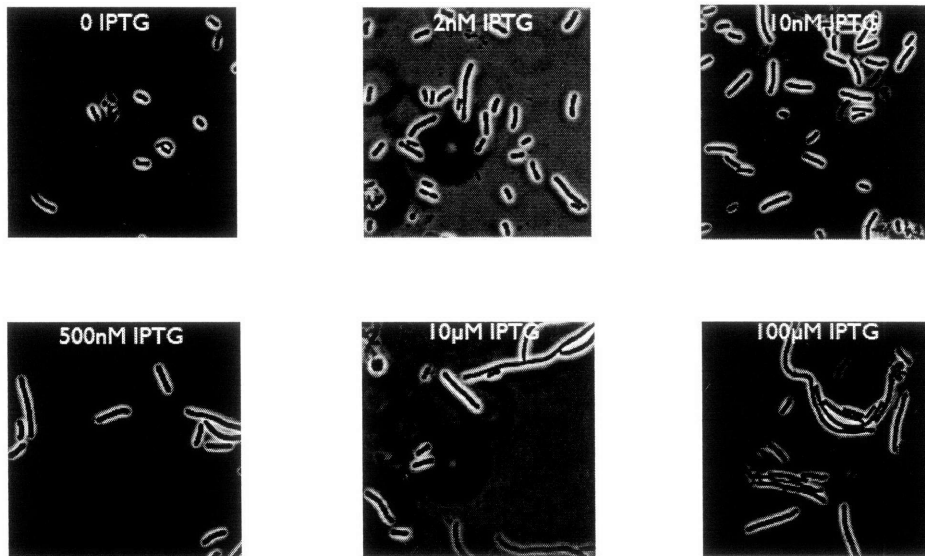


FIG. 6.13: Images of Avo123 after they have been grown for a week in different concentrations of IPTG.

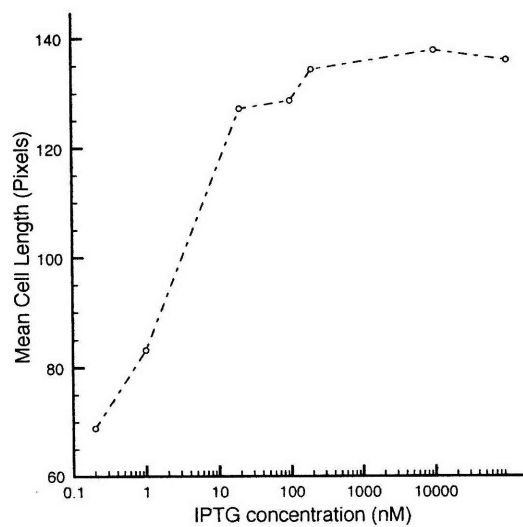


FIG. 6.14: Mean lengths of Avo123 after they have been grown for a week in different concentrations of IPTG.

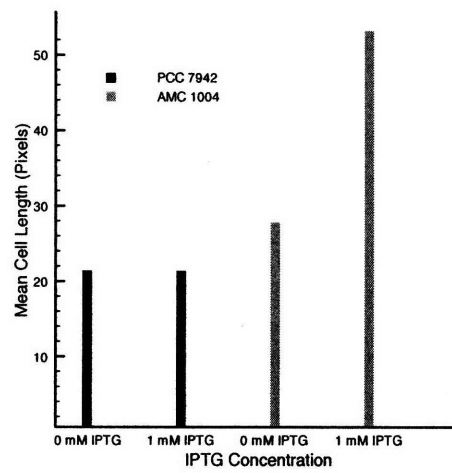


FIG. 6.15: Increase in cell length observed for strain AMC1004 after induction with 1mM IPTG.

Chapter 7

Conclusion

Circadian clocks are ubiquitous in eukaryotic organisms and the preferred mechanism of operation of these clocks is the transcription-translation oscillator or TTO. Oscillators such as these, based on delayed negative feedback, have been well studied and even synthesized [23]. The circadian oscillations in cyanobacteria are unique in several ways: (a) Cyanobacteria are the simplest known organisms to have a circadian clock [24] (b) Cyanobacteria negate the 'circadian-infradian' hypothesis - the idea that any organism that divides at a rate faster than once in 24 hours could not maintain a circadian rhythm, and (c) The oscillations in cyanobacteria can be generated by interactions between only three proteins and do not require any genetic feedback.

As such, cyanobacteria offer a unique opportunity to investigate how complex behavior such as oscillations can arise simply due to protein-protein interactions between just three proteins. In this regard, numerous experiments have been carried out and models constructed to try and understand the interactions between the Kai proteins *in vitro*. This work is one that attempts to understand the behavior of the Kai proteins *in vivo*. Using YFP (yellow fluorescent protein) tagged to the Kai proteins, it was discovered that all three Kai proteins localize to one of the poles of the cell. It was also discovered that the localization of the protein KaiA is dependent on the presence of the other proteins KaiB and KaiC while KaiB localizes to the pole on its own independent of the other proteins. If we assume that polar localization could be a result of preferential association of KaiB with the cell membrane at the cell pole then this discovery is in good agreement with the finding that the majority of KaiB is present in the cell membrane at all times [25]. Furthermore, it was discovered that the phosphorylation state of KaiC determined the localization of KaiA. Specifically, KaiA is localized to the cell pole only if KaiC is phosphorylated at the Ser431 phosphorylation site. It is known from *in vitro* experiments that the Kai proteins form a large molecular weight complex during the second half of the circadian cycle when the phosphorylation level of KaiC is high. This indicates that the observed localization of KaiA at the cell pole could well be the manifestation of the KaiA-B-C complex. The results of our experiments would then indicate that the three-protein complex is largely restricted to the cell pole.

It was surmised that the aggregation of the Kai proteins at the pole of the cell could have a role in regulating cell division in cyanobacteria. It was discovered in a previous study that the circadian clock of cyanobacteria governs its cell division cycle [26]. In our work, we found that indeed when KaiA is overexpressed in a cell so that it is localized, cell division is inhibited and the cyanobacteria show a much longer length than normal. This is in agreement with the previous finding that cell division in cyanobacteria appeared to be inhibited during times of peak KaiC phosphorylation. Since KaiA enhances KaiC

phosphorylation, it would follow that overexpressing KaiA would inhibit cell division. Normal cell division is restored when the induction is removed.

Time-lapse experiments were conducted to ascertain if there was a preferred pole of localization for overexpressed KaiB. Specifically, to find out whether the localization occurred at the new poles or at the old poles after cell division. Such a pole preference would lend strong support to the hypothesis that the localization plays a role in regulating cell division. Experiment showed, however, that there was no preferred pole of localization. In this work, it was established that localization of KaiA depends on the phosphorylation state of KaiC. It is well known that the basis of the cyanobacterial circadian oscillator is the phosphorylation cycle of KaiC. The phosphorylation level of KaiC oscillates with a 24 hour period due to its interactions with the other Kai proteins and ATP. Since the localization of KaiA depends on the phosphorylation state of KaiC and the phosphorylation state of KaiC oscillates with a 24 hour period, it was reasonable to think that the localization of KaiA would also oscillate with a 24 hour period. Since it was not possible to measure the localization of KaiA as a function of time because overexpression of KaiA (necessary for the observation of localization) abolished the circadian rhythm, the localization of KaiC as a function of time was measured instead using several different strains. Knowing whether such an oscillation existed would be very useful in attempting to decipher the nature and function of the localization. While preliminary experiments with an arrhythmic KaiCYFP fusion strain indicated the presence of such oscillations, subsequent experiments with functional strains failed to confirm that observation. To the precision of the apparatus and methods used, it appears that the localization of KaiCYFP does not oscillate with time.

It would be very interesting to use fluorescent proteins of different colors to tag the Kai proteins and measure co-localization. While it is not possible to use red fluorescent protein (RFP) for this purpose, CFP (cyan fluorescent protein) is a potential candidate. It would also be very useful to fluorescently tag the FtsZ protein (involved in cell septation at the time of division) to observe its behavior during KaiA overexpression when cell division is inhibited. The behavior of the phospho-mimetic mutants of KaiC, namely the functionality of their circadian clocks also needs to be ascertained.

Bibliography

- [1] R. Ward, "Living Clocks", Knopf, New York 1971.
- [2] J.W. Schopf and B.M. Packer, "Early Archean (3.3-billion to 3.5-billion-year-old) microfossils from Warrawoona Group, Australia", *Science*, **237**, pp. 70 -73 (1987).
- [3] A. Mitsui et. al., "Strategy by which nitrogen-fixing unicellular cyanobacteria grow photoautotrophically", *Nature*, **323** , pp. 720 - 722 (1986).
- [4] T.Kondo et. al., "Circadian Rhythms in Prokaryotes: Luciferase as a Reporter of Circadian Gene Expression in Cyanobacteria", *PNAS*, **90**, pp. 5672-5676 (1993).
- [5] Y. Kitayama et. al. , "KaiB functions as an attenuator of KaiC phosphorylation in the cyanobacterial circadian clock system", *EMBO J.*, **22**, pp. 2127-2134 (2003).
- [6] C. R. McClung, "The cyanobacterial circadian clock is based on the intrinsic ATPase activity of KaiC", *PNAS*, **104**, pp. 16727-16728 (2007).
- [7] J. Tomita et. al., "No Transcription-Translation Feedback in Circadian Rhythm of KaiC Phosphorylation", *Science*, **307**, pp. 251 - 254 (2005).
- [8] M. Nakajima et. al., "Reconstitution of Circadian Oscillation of Cyanobacterial KaiC Phosphorylation in Vitro", *Science*, **308**, pp. 414-415 (2005).
- [9] S. Williams et. al., "Structure and Function from the Circadian Clock Protein KaiA of *Synechococcus Elongatus*: A Potential Clock Input Mechanism", *PNAS*, **99** , pp. 15357-15362 (2002).
- [10] P. Wolanin et. al., "Histidine Protein Kinases: Key Signal Transducers Outside the Animal Kingdom", *Genome Biology*, **3** , pp. 3013.1 - 3013.8 (2002).
- [11] I. Vakonakis and A.C. LiWang, "Structure of the C-terminal domain of the clock protein KaiA in complex with a KaiC-derived peptide: Implications for KaiC regulation", *PNAS*, **101** , pp. 10925-10930 (2004).
- [12] F. Hayashi et. al., "Roles of Two ATPase-Motif-containing Domains in Cyanobacterial Circadian Clock Protein KaiC", *J. Biol. Chem.*, **279** , pp. 52331-52337 (2004).
- [13] E. Emlerly, N.S. Wingreen, "Hourglass Model for a Protein-Based Circadian Oscillator", *Physical Review Letters*, **96**, pp. 03803-01 - 03803-4 (2006).
- [14] J.R. Chabot et. al., "Stochastic gene expression out-of-steady-state in the cyanobacterial circadian clock", *Nature*, **450**, pp. 1249 - 1252 (2007).

- [15] J.R. Chabot, "Genetic noise in the cyanobacterial circadian oscillator", Ph.D. thesis MIT (2005).
- [16] P. Kovesi, "Phase Preserving Denoising of Images", *The Australian Pattern Recognition Society Conference: DITA '99* . Perth WA, pp 212 - 217 (1999).
- [17] T. Nishiwaki et. al., "A sequential program of dual phosphorylation of KaiC as a basis for circadian rhythm in cyanobacteria", *EMBO Journal*, **26** , pp. 4029 - 4037 (2007).
- [18] H. Kageyama et. al., "Cyanobacterial Circadian Pacemaker: Kai Protein Complex Dynamics in the KaiC Phosphorylation Cycle In Vitro", *Molecular Cell*, **23** , pp. 161-171 (2006).
- [19] M.J. Rust et. al., "Ordered Phosphorylation Governs Oscillation of a Three-Protein Circadian Clock", *Science*, **318**, pp. 809 - 812 (2007).
- [20] W.F. Doolittle, "The Cyanobacterial Genome, its Expression, and the Control of that Expression", *Adv. Microb. Physiol.*, **20** , pp. 1-102 (1979).
- [21] H. Kageyama, T. Kondo, H. Iwasaki, "Circadian Formation of Clock Protein Complexes by KaiA, KaiB, KaiC, and SasA in Cyanobacteria", *Journal of Biological Chemistry*, **278 -4**, pp. 2388 - 2395 (2003).
- [22] H. Kageyama et. al., "Cyanobacterial Circadian Pacemaker: Kai Protein Complex Dynamics in the KaiC Phosphorylation Cycle In Vitro", *Molecular Cell*, **23** , pp. 161 - 171 (2006).
- [23] M.B. Elowitz and S. Leibler, "A Synthetic Oscillatory Network of Transcriptional Regulators", *Nature*, **403** , pp. 335 -338.
- [24] H.Iwasaki and T. Kondo, "The Current State and Problems of Circadian Clock Studies in Cyanobacteria", *Plant and Cell Physiology*, **41** , pp. 1013-1020 (2000).
- [25] Y. Kitayama et. al., "KaiB functions as an attenuator of KaiC phosphorylation in the cyanobacterial circadian clock system", *EMBO J.*, **22** , pp. 2127 - 2134 (2003).
- [26] T. Mori, B. Binder and C.H. Johnson, "Circadian gating of cell division in cyanobacteria growing with average doubling times of less than 24 hours", *PNAS*, **93**, pp. 10183 - 10188 (1996).